

**Grid Integration of Offshore Wind Power
Standards, Control, Power Quality and Transmission**

Wu, Dan; Seo, Gab-Su; Xu, Lie ; Su, Chi; Kocewiak, Łukasz ; Qin, Zian

DOI

[10.1109/OJPEL.2024.3390417](https://doi.org/10.1109/OJPEL.2024.3390417)

Publication date

2024

Document Version

Final published version

Published in

IEEE Open Journal of Power Electronics

Citation (APA)

Wu, D., Seo, G.-S., Xu, L., Su, C., Kocewiak, Ł., & Qin, Z. (2024). Grid Integration of Offshore Wind Power: Standards, Control, Power Quality and Transmission. *IEEE Open Journal of Power Electronics*, 5, 583-604. <https://doi.org/10.1109/OJPEL.2024.3390417>

Important note

To cite this publication, please use the final published version (if applicable).
Please check the document version above.






Copyright

Other than for strictly personal use, it is not permitted to download, forward or distribute the text or part of it, without the consent of the author(s) and/or copyright holder(s), unless the work is under an open content license such as Creative Commons.

Takedown policy

Please contact us and provide details if you believe this document breaches copyrights.
We will remove access to the work immediately and investigate your claim.

Grid Integration of Offshore Wind Power: Standards, Control, Power Quality and Transmission

DAN WU ¹ (Senior Member, IEEE), GAB-SU SEO ² (Senior Member, IEEE),
LIE XU ³ (Senior Member, IEEE), CHI SU⁴, LUKASZ KOCEWIAK ⁵ (Senior Member, IEEE),
YIN SUN³ (Member, IEEE), AND ZIAN QIN ⁶ (Senior Member, IEEE)

¹Shell Global Solution International B.V., 2288 GK Rijswijk, The Netherlands

²Power Systems Engineering Center, National Renewable Energy Laboratory, Golden, CO 80401 USA

³University of Strathclyde, Glasgow G1 1XW, U.K.

⁴Siemens Gamesa, 2820 Gentofte, Denmark

⁵Orsted, 2820 Gentofte, Denmark

⁶Delft University of Technology, 2628CD Delft, The Netherlands

CORRESPONDING AUTHOR: GAB-SU SEO (e-mail: gabsu.seo@nrel.gov)

This work was supported in part by the National Renewable Energy Laboratory, operated by Alliance for Sustainable Energy, LLC, for the U.S. Department of Energy (DOE) under Contract Number DE-AC36-08GO28308, in part by the U.S. Department of Energy Office of Energy Efficiency and Renewable Energy under the Solar Energy Technologies Office Award Number 38637, and in part by the Grid Modernization Initiative of DOE's part of its Grid Modernization Laboratory Consortium, a strategic partnership between DOE and the national laboratories to bring together leading experts, technologies, and resources to collaborate on the goal of modernizing the nation's grid.

ABSTRACT Offshore wind is expected to be a major player in the global efforts toward decarbonization, leading to exceptional changes in modern power systems. Understanding the impacts and capabilities of the relatively new and uniquely positioned assets in grids with high integration levels of inverter-based resources, however, is lacking, raising concerns about grid reliability, stability, power quality, and resilience, with the absence of updated grid codes to guide the massive deployment of offshore wind. To help fill the gap, this paper presents an overview of the state-of-the-art technologies of offshore wind power grid integration. First, the paper investigates the most current grid requirements for wind power plant integration, based on a harmonized European Network of Transmission System Operators (ENTSO-E) framework and notable international standards, and it illuminates future directions. The paper discusses the wind turbine and wind power plant control strategies, and new control approaches, such as grid-forming control, are presented in detail. The paper reviews recent research on the ancillary services that offshore wind power plants can potentially provide, which, when harmonized, will not only comply with regulations but also improve the value of the asset. The paper explores topics of wind power plant harmonics, reviewing the latest standards in detail and outlining mitigation methods. The paper also presents stability analysis methods for wind power plants, with discussions centered on validity and computational efficiency. Finally, the paper discusses wind power plant transmission solutions, with a focus on high-voltage direct-current topologies and controls.

INDEX TERMS Offshore wind power, inverter-based resources, grid-forming inverter, inverter ancillary service, power quality, stability analysis.

I. INTRODUCTION

Wind energy integration plays a vital role in achieving the net-zero emissions goals. Although land-based wind turbines still dominate the total cumulative wind power capacity in the wind energy market, the offshore wind industry has

dramatically grown during the last 30 years. Starting with the Vindeby offshore wind power plant, which was commissioned in Denmark in 1991, the world's first offshore wind power plant was mostly considered a demonstration project of 5 MW total, supplying electricity to 2,200 households, and

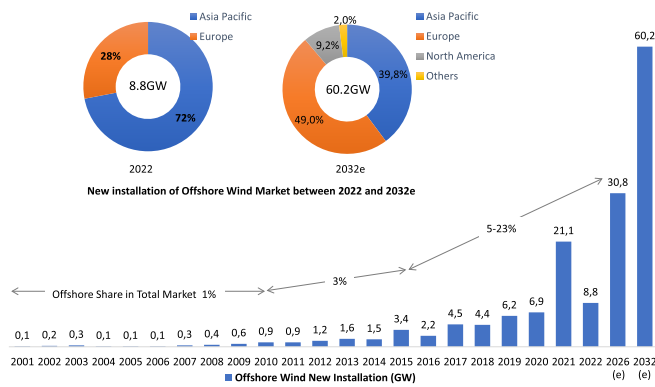


FIGURE 1. Offshore global market status [2].

the early-stage offshore wind market was limited to only a few scattered European countries. As of 2023, the world's largest AC-connected offshore wind power plant, Hornsea II, is fully in operational in the United Kingdom, with 1.386 GW total, powering 1.3 million homes, and the offshore wind market is becoming global [1]. Fig. 1 shows the new global offshore wind installations during the past decades and their market share from 2022 to 2032 (expected) [2]. Besides political reasons for a more worldwide focus on decarbonization to mitigate climate change, one technical incentive behind this fast growth is that offshore wind generation more efficiently uses wind energy and has fewer environmental impacts than its land-based counterpart, and thus the wind turbine generator (WTG) can be designed with a larger rotor size and power capacity. As WTG manufacturers and offshore wind power plant (OWPP) developers are competing for the larger wind turbine and wind power plant capacity, how to ensure good grid connection performance is a critical topic. For example, reference [3] discusses various instability incidents found in the industry, including the German North Sea OWPP oscillation connected with the HVDC link and other incidents found in the application of Type 3 and Type 4 turbines.

In [4], the authors point out that grid integration ranks as one of the most challenging topics the wind industry faces in both the short (next 5 years) and long term (10 years and beyond). On the one hand, regional grid codes and international standards are subject to continuous changes, making it challenging for manufacturers and developers to timely adapt to the diverse and strict grid requirements during the development of WTGs in commercial projects. In addition, grid operators require OWPPs to not only fulfill grid codes but also contribute to improving grid resilience and provide ancillary services. On the other hand, the increased capacity and the location of OWPPs farther from shore bring challenges in terms of i) weaker grid connections and ii) power transmission over longer distances. The former issue urges WTG manufacturers to improve converter controller design to ensure stable operation, and performing stability analysis of the OWPP integration with the main grid tends to be a mandatory step for developers during the wind power plant

design. The latter issue makes the high-voltage direct-current (HVDC) connection a popular and more efficient solution in modern, large OWPP projects than the traditional counterpart, high-voltage alternating-current (HVAC), which takes up higher reactive power along transmission cables.

The challenges of grid integration with the fast-paced development of offshore wind have drawn significant attention from academia and industry. Recently published review papers outlined the wind power technology, focusing on WTG topology and wind power plant infrastructure, briefly summarizing grid integration in [5], [6], respectively, and OWPP grid integration in [7]. Nevertheless, some critical emerging topics that have drawn tremendous attention from industry and academia are missing, such as the black-start capability of WTGs or OWPPs, grid-forming (GFM) inverter technology, and recent cutting-edge HVDC developments. Thus, the motivation of this paper is to go a step further in overviewing the state of the art of grid integration technology from both academic and industry perspectives, starting with a screening of grid codes, in particular, using the European harmonized grid code framework as an example, and highlighting the power quality requirements in standards. We explore WTG and wind power plant control strategies by investigating the currently dominant grid-following (GFL) control and the future promising GFM control. We also discuss ancillary services, such as black start and virtual inertia, which have been taken as technology enablers to realize and improve grid resilience and are closely influenced by controller design. In addition, this paper distinctively explains the harmonics and stability aspects because they remain some of the most challenging aspects when evaluating OWPP grid connection performance. Finally, we present an overview of the HVDC topology and control since they are shown to be the most promising transmission solutions for the future long-distance, large-scale deployment of OWPPs.

II. GRID CODES AND STANDARDS TO SUPPORT WIND POWER PLANT GRID INTEGRATION

Grid codes outline the technical requirements and responsibilities for both generators and loads that are connected to the transmission or distribution systems. The requirements differ from one country to another, and in some countries, such as the United States and Japan, there can be several entities that regulate the respective regional codes. In Europe, the European Network of Transmission System Operators for Electricity (ENTSO-E), which comprises 39 transmission system operators (TSOs) (as of 2023), has made good progress toward harmonizing the grid codes that outline the requirements across five synchronous regions with the ENTSO-E Requirements for Generators (ENTSO-E RfG) [8]. In this section, we use the framework of ENTSO-E RfG to illustrate the grid codes in Europe together with examples of representative TSOs of countries with high wind integration levels. In addition, we discuss the requirements in select countries with emerging offshore wind markets, including the United States, Taiwan, and Japan. The overview of the grid code

TABLE 1. Overview of Grid Code Examples

Market	Country/Region	Area	TSO/Association	Grid Code
EU Market	Denmark	Nordic	Energinet	[9]
	Germany	Central Europe	Tennet	[10]
	United Kingdom	U.K.	National Grid	[11]
	Ireland	Ireland and Northern Ireland	EirGrid	[12]
	EU	EU	ENTSO-E	[8]
Emerging Market	Taiwan	APAC	Taipower	[13]
	Japan	APAC	Japan Electric Association	[14]
	North America	North America	FERC, NERC*	[15]

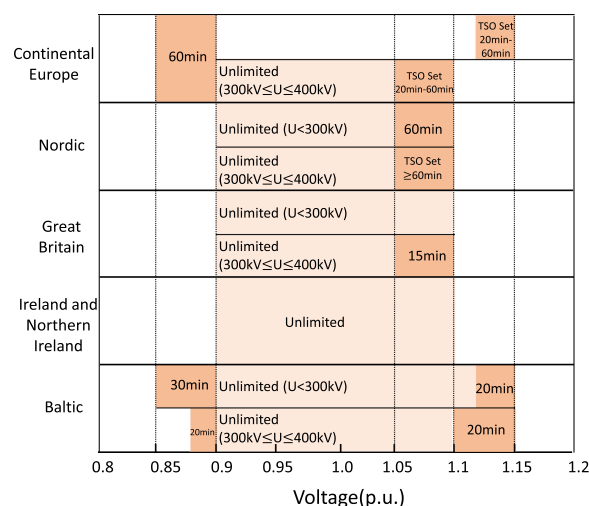
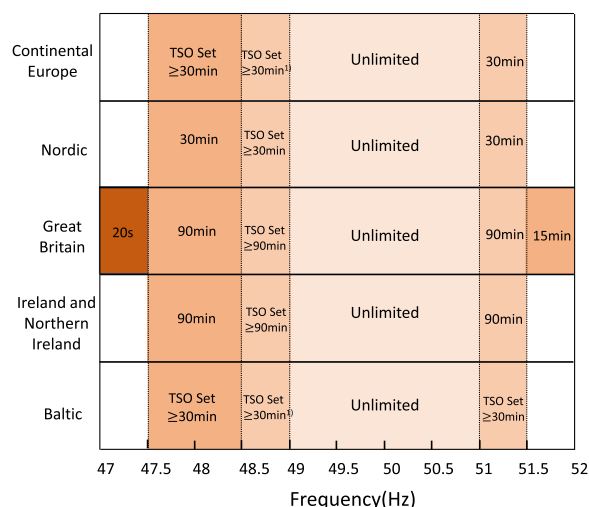


FIGURE 2. Frequency and voltage tolerance requirements in ENTSO-E. To be specified by each TSO but not less than the period for 47.5 Hz–48.5 Hz).

examples presented in this paper is shown in Table 1. Power quality requirements are not normally found in grid codes but rather originate from IEC and IEEE standards. These are also discussed in detail.

A. FREQUENCY AND VOLTAGE TOLERANCE

The frequency and voltage operating ranges are the most basic requirements for OWPPs to remain connected to the grid. Fig. 2 shows the requirements of the ENTSO-E RfG. A more detailed comparison can be found in [16], [17]. In

the emerging wind energy market, Taiwan recently amended the frequency operating range requirement in 2021 [13], compared to the 2009 precedent, which specified only the voltage tolerance range requirement of 0.9 pu to 1.1 pu. In the United States, there is no unified grid code that is applied to all regions, although the North American Electric Reliability Corporation (NERC), an organization similar to ENTSO-E, has summarized the requirements in its standard [15].

In addition to the static frequency limit, some grid codes also require that the OWPP should withstand up to a certain rate of change of frequency (RoCoF). Although ENTSO-E has not included unified requirements for synchronous regions, such requirements can be found in individual grid codes, e.g., Denmark [9] and Germany [10] require 2.5 Hz/s, and Great Britain requires 2.5 Hz/s and 1 Hz/s for DC- and AC-connected OWPPs, respectively [11].

B. ACTIVE POWER AND FREQUENCY CONTROL

Both active power and frequency control contribute to the frequency stability of wind power plants. Active power control requires OWPPs to be able to regulate their active power injection at the maximum power available or at a set point with a predefined ramping rate. This can be achieved by either a direct external set point or a percentage of the available power as spinning reserve.

The frequency control, according to the ENTSO-E RfG, has three operation modes: limited frequency sensitive mode – overfrequency (LFSM-O), limited frequency sensitive mode – underfrequency (LFSM-U), and frequency sensitive mode (FSM), as shown in Fig. 3. Whereas LFSM-O only requires the OWPP to curtail power in an overfrequency event, LFSM-U and FSM need the OWPP to increase power during underfrequency events, meaning the OWPP should derate the power generation from the maximum available power at nominal frequency so that some headroom is reserved for the power boost in case of a frequency contingency. Long-term power derating can lead to an increase in the levelized cost of energy, and therefore whether to activate this function is a question of balancing economic aspects and system stability for wind power plant developers [17]. Depending on the combination of on/off active power control and frequency control, OWPPs can be operated with different control responses, for example, as per Ireland’s grid code [12]. In Fig. 3, the 100% available active power (AAP) curve means that the OWPP operates at 100% AAP at nominal frequency, which can be analogous to LFSM-O when there is an overfrequency event. To perform

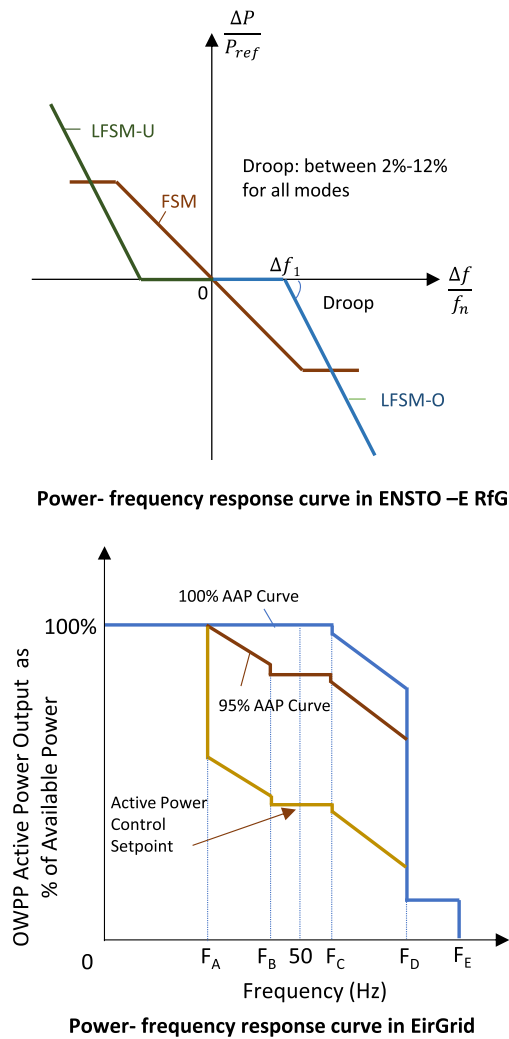


FIGURE 3. Frequency control mode requirement from the ENSTO-E RfG and EirGrid. Δf is the frequency deviation from the nominal frequency f_n ; ΔP is the regulated power of the frequency control; P_{ref} is the maximum power capacity; and Δf_1 is the frequency insensitive limits.

the FSM response, the OWPP needs to derate to a 95% AAP curve (with the default 5% spinning reserve) or be controlled at an external active power set point that is lower than the maximum power of 50 Hz.

C. REACTIVE POWER AND VOLTAGE REGULATION

Similar to active power and frequency regulation contributing to frequency stability, the reactive power regulation of OWPPs contributes to the voltage stability of the grid. There are two major topics of voltage stability in grid codes: i) reactive power capability and ii) reactive power controllability. U-Q and P-Q diagrams are typically used to present reactive power capability, as shown in Fig. 4 for Germany, Denmark, and the United Kingdom, and Ireland. Note that the curves represent the selective cases of the requirements. For instance, the U.K. plot represents a more restrictive case for the meshed grid connection for OWPPs (Configuration 2 in the grid code).

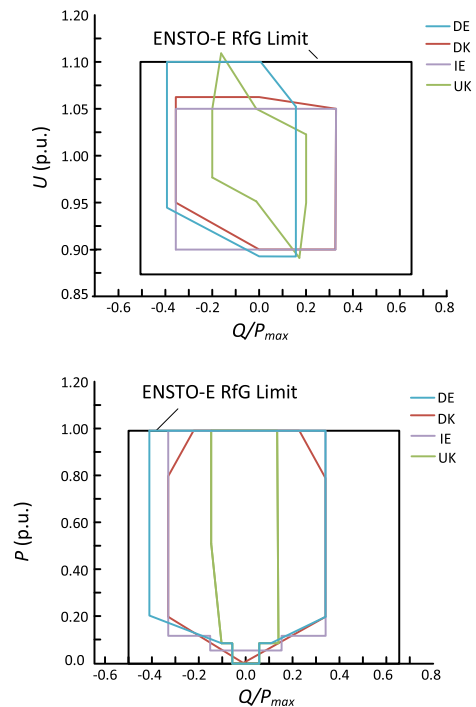
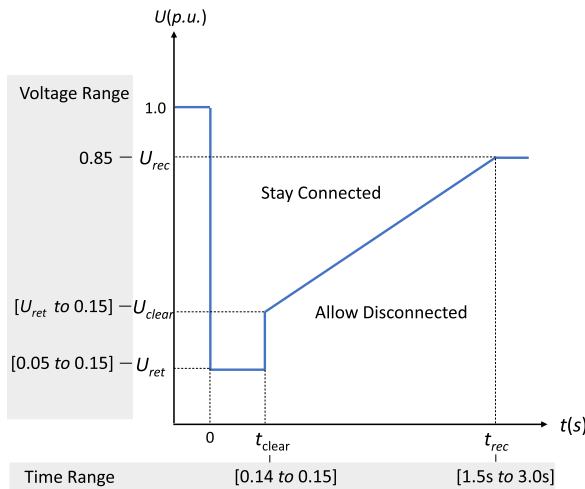


FIGURE 4. U-Q and P-Q capability requirement comparison.

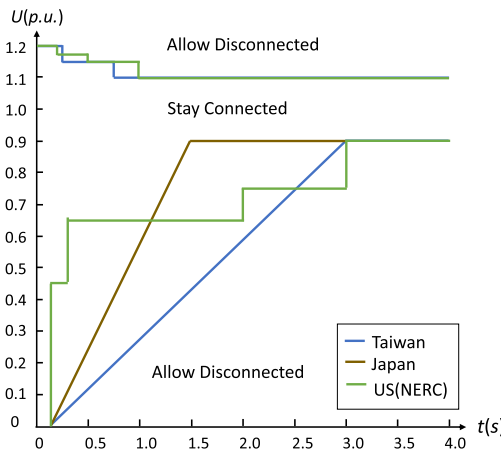
In Configuration 1 (OWPP connected to only one onshore substation), the current U.K. grid code (Issue 5 at the time of writing) states only the minimum capability of zero reactive power transfer to the grid. In Fig. 4, the outer boundary is set by the ENSTO-E RfG, which defines the maximum capability, and individual national/regional TSOs reshape the envelope according to their specific grid conditions. To meet the reactive power capability and ensure the reliable operation of OWPPs, the developers need to consider holistic wind power plant design, such as WTG reactive power capability, equipment voltage and current limitation, and cable charging reactive power during the energizing process. Reactive power compensation is usually achieved by various types of reactive power compensation equipment, such as (fixed/variable) shunt reactors and STATCOM, together with WTG-inherent PQ capability. With respect to reactive power controllability, three control modes are defined in most grid codes: i) reactive power control mode, ii) power factor control mode, and iii) voltage control mode. Reactive power controllability requires that the OWPP be able to control the reactive power in a direct manner by receiving external set points in reactive power and power factor control modes or in an indirect way with a voltage reference and predefined V-Q slope in voltage control mode.

D. FAULT RIDE-THROUGH CAPABILITY

Fault ride-through (FRT) capability includes two parts: low-voltage ride-through (LVRT) and high-voltage ride-through (HVRT). The LVRT capability is one of the most basic and oldest requirements included in most grid codes. It requires



FRT requirement in ENSTO-E RfG



FRT requirement in Emerging Market Examples

FIGURE 5. FRT requirements in the ENSTO-E RfG and emerging markets (U_{ret} is the retained voltage during the fault, U_{clear} is the voltage when the fault is cleared at t_{clear} , and U_{rec} is the lower limit of the voltage recovery at time t_{rec}).

OWPPs to stay grid-connected for a minimum period of time when a nearby system experiences a short circuit. Similarly, the HVRT function is required for OWPPs to ride through temporary overvoltage situations, which can be caused by switching events, lightning strikes, or voltage volatility due to insufficient grid strength. Currently, there is not yet a specific requirement in the ENSTO-E RfG, leaving this for individual TSOs to complement, if needed. Fig. 5 summarizes the FRT requirements of the ENSTO-E RfG and emerging markets.

In addition to the FRT curve, there are further requirements in grid codes for the performance of OWPPs during and after a fault, including reactive current injection, active power or reactive power prioritization during a fault, active power recovery, and sequential fault handling. Some of these requirements are briefly mentioned in the ENSTO-E RfG,

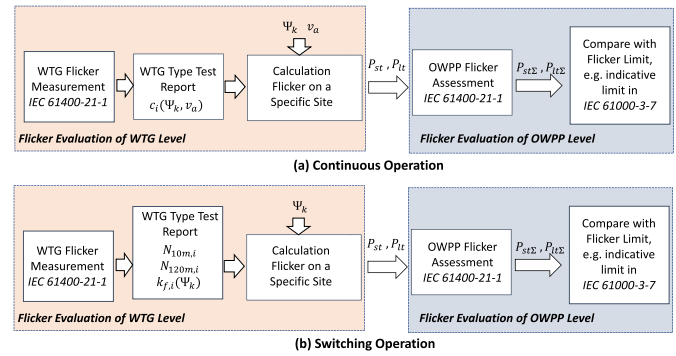


FIGURE 6. Flicker evaluation according to IEC 61400-21-1 [18].

but detailed specifications differ among national/regional grid codes. The most typical is the reactive current injection, which can facilitate voltage support. An in-depth understanding of these additional requirements should be treated on a case-by-case basis in grid codes. For example, a grid code could determine whether the voltage dip should use the minimum voltage or positive-sequence voltage when detecting a fault or whether the reactive current injection should be solely dependent on a voltage dip or another current in addition to the pre-fault one.

E. POWER QUALITY REQUIREMENTS

The most concerning power quality requirements of OWPPs are flicker and harmonics. Flicker refers to the rapid voltage change (higher than six times per hour) that can cause incandescent lamps to illuminate unsteadily. Flicker emissions of OWPPs are evaluated for continuous operation and switching operation during the WTG startup or when switching between generators; the process is shown in Fig. 6. The total OWPP flicker evaluation starts from individual WTG flicker calculations. For continuous operation, the flicker coefficient, $c_i(\Psi_k, v_a)$, for each turbine can be identified based on the WTG type test report, where Ψ_k is the grid impedance phase angle, and v_a is the annual wind speed. Considering multiple WTGs connected to the point of connection (PoC), the continuous flicker emissions from the sum of the turbines can be estimated according to IEC 61400-21-1 [18]:

$$P_{st\Sigma} = P_{lt\Sigma} = \frac{1}{S_k} \sqrt{\sum_{i=1}^{N_{wt}} (c_i(\Psi_k, v_a) \times S_{n,i})^2} \quad (1)$$

where P_{st} and P_{lt} are the short-term and long-term flicker emissions, respectively; $S_{n,i}$ is the rated apparent power of the individual wind turbine; S_k is the short-circuit apparent power at the PoC; and N_{wt} is the number of WTGs connected to the PoC.

For switching operations, the flicker emissions from the sum of the turbines can be estimated as [18]:

$$P_{st\Sigma} = \frac{18}{S_k} \times \left(\sum_{i=1}^{N_{wt}} N_{10\ m,i} \times (k_{f,i}(\Psi_k) \times S_{n,i})^{3.2} \right)^{0.31} \quad (2)$$

TABLE 2. Indicative Planning Levels Defined in IEC 61000-3-6: 2008 for Harmonic Voltages in Power Systems (>35 Kv)

Odd harmonics non-multiples of 3		Odd harmonics multiples of 3		Even harmonics	
Harmonic order h	Harmonic voltage %	Harmonic order h	Harmonic voltage %	Harmonic order h	Harmonic voltage %
5	2	3	2	2	1.4
7	2	9	1	4	0.8
11	1.5	15	0.3	6	0.4
13	1.5	21	0.2	8	0.4
$17 \leq h \leq 49$	$1.2 \cdot \frac{17}{h}$	$21 \leq h \leq 45$	0.2	$10 \leq h \leq 50$	$0.19 \cdot \frac{10}{h} + 0.16$

The indicative planning levels for the total harmonic distortion are THD = 3%.

TABLE 3. Current Distortion Limits Defined in IEEE 519 for Systems Rated Above 69 Kv Through 161 Kv

Maximum harmonic current distortion in percentage of I_L							
Individual harmonic order (odd harmonics) ^{a,b}							
System rated voltage	I_{sc}/I_L	$3 \leq h < 11$	$11 \leq h < 17$	$17 \leq h < 23$	$23 \leq h < 35$	$35 \leq h < 50$	TDD
$> 69kV, \leq 161kV$	$< 20^c$	2.0	1.0	0.75	0.3	0.15	2.5
	20 ~ 50	3.5	1.75	1.25	0.5	0.25	4.0
	50 ~ 100	5.0	2.25	2.0	0.75	0.35	6.0
	100 ~ 1000	6.0	2.75	2.5	1.0	0.5	7.5
	> 1000	7.5	3.5	3.0	1.25	0.7	10.0
$> 161kV$	$< 25^c$	1.0	0.5	0.38	0.15	0.1	1.5
	25 ~ 50	2.0	1.0	0.75	0.3	0.15	2.5
	≤ 50	3.0	1.5	1.15	0.45	0.22	3.75

^a Even harmonics are limited to 25% of the odd harmonic limits noted here.

^b Current distortions that result in a DC offset, e.g., half-wave converters, are not allowed.

^c All power generation equipment is limited to these values of current distortion, regardless of actual I_{sc}/I_L ,

where:

I_{sc} = maximum short-circuit current at PCC

I_L = maximum demand load current (fundamental frequency component at the PCC under normal load operating conditions).

$$P_{lt\Sigma} = \frac{8}{S_k} \times \left(\sum_{i=1}^{N_{wt}} N_{120\ m,i} \times (k_{f,i}(\Psi_k) \times S_{n,i})^{3.2} \right)^{0.31} \quad (3)$$

where $N_{10\ m,i}$ and $N_{120\ m,i}$ are the number of switching operations of individual wind turbines within a 10-minute and 2-hour period, respectively; and $k_{f,i}(\Psi_k)$ is the flicker step factor of the individual wind turbines, abstracted from the individual WTG type test report.

Finally, the total OWPP flicker emissions of both continuous and switching operations should be compared and should be below the planning level limits determined by the TSO; according to IEC 61000-3-7 [19], such indicative limits are $P_{st} = 0.8$ and $P_{lt} = 0.6$, respectively, for voltage levels higher than 35 kV.

Harmonics are voltages and currents that have frequencies that are integer (typical harmonics) or noninteger (interharmonics) multiples of the fundamental. They can be problematic because of, but not limited to, the following reasons: i) The harmonic current injected into the grid can induce harmonic voltages in the grid; ii) the harmonic current can interfere with the communication systems; and/or iii) the harmonic current can damage or speed up the aging of the components in the grid infrastructure [20]. Thus, an OWPP, as any other grid-connected source or load, must fulfill the harmonic requirements.

When an OWPP requests connection to the grid, the grid operator will give permission only if the harmonics level at the PoC is kept below the level regulated upon connection of the OWPP. Indicative planning levels for harmonic voltages per order are defined in IEC 61000-3-6, as shown in Table 2. IEEE 519 gives the harmonic current limits and the limits of the

TABLE 4. Voltage Distortion Limits Defined in IEEE 519

Bus voltage (V) at PCC	Individual harmonic (%)	Total harmonic distortion (THD) (%)
$69kV < V \leq 161kV$	1.5	2.5
$161kV < V$	1.0	1.5 ^a

^a High-voltage systems can have up to 2.0% THD where the cause is an HVDC terminal whose effects will have attenuated at points in the network where future users may be connected.

voltage total harmonic distortion (THD) per order, as shown in Table 3 and 4.

For the harmonic emissions evaluation, the traditional method is to abstract the WTG output harmonic voltage/current from the WTG measurement campaign, as presented in the previous version of IEC 61400-21-3, before its revision in 2019; however, this method does not consider the impact of grid conditions on the WTG terminal voltage. The 2019 version of IEC 61400-21-3 [21] recommends that the harmonic model establish WTG harmonic emissions to separate the harmonics produced by the WTGs and the harmonics from the distorted grid, as shown in Fig. 7, where U_{h_out} and I_{h_out} are the WTG measured terminal harmonic output voltage and current, respectively, and U_{h_WTG} and Z_{h_WTG} are the WTG harmonic voltage source and impedance, which are independent from the grid conditions.

III. WIND TURBINE AND WIND POWER PLANT CONTROL FOR GRID INTEGRATION

The power converter of offshore wind turbines usually has a back-to-back structure, as shown in Fig. 8, to perform an AC-DC-AC power conversion [22], [23]. Although AC-AC

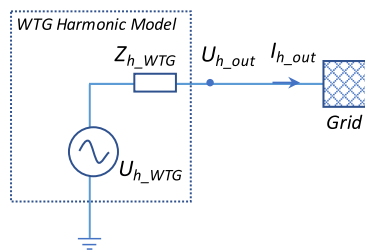


FIGURE 7. Harmonic model of wind turbines.

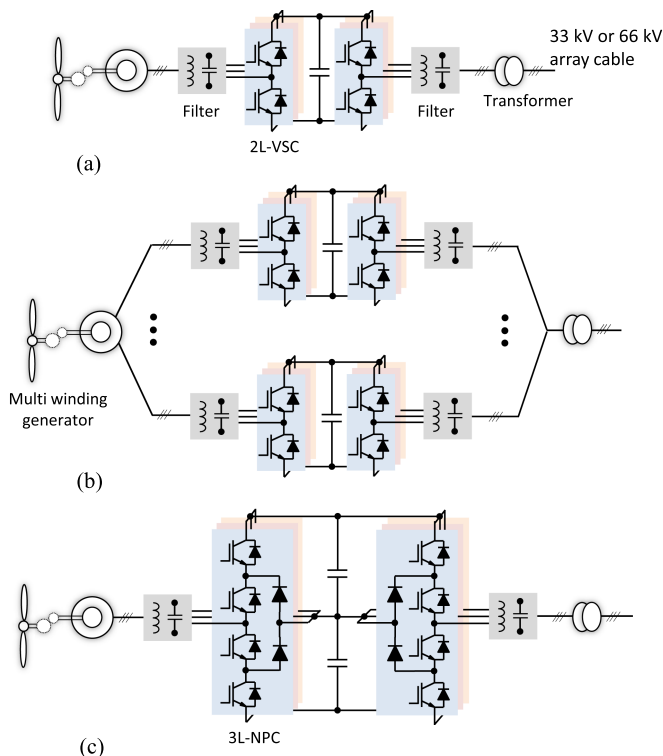


FIGURE 8. Offshore wind power converter topologies: (a) two-level back-to-back converter, (b) parallel-connected two-level back-to-back converter, and (c) three-level NPC back-to-back converter.

power converters are discussed in the literature and exist in some applications, a DC link is still retained to isolate the generator from the grid fault and enhance its grid fault ride-through capability. For small wind turbines, the front-end AC-DC converter can be a diode rectifier or a diode-bridge-based power factor correction circuit. For large-scale offshore wind turbines, active bridges are the mainstream for higher controllability. Current source inverters have advantages such as short-circuit protection. Nonetheless, their performance significantly degrades when the load is light. Voltage source inverters are, therefore, still dominant in large-scale wind turbines. The two-level converter, as depicted in Fig. 8(a), is adequate when the DC-link voltage is around 1200 V and the grid side is 690 V. It also takes advantage of the technology maturity and relatively low cost of the low-voltage power electronics. Despite this, the power rating of offshore

wind turbines keeps increasing, e.g., GE Haliade-X rated at 14 MW and Siemens Gamesa SG 14–222 DD rated at 14 MW. Multi-two-level back-to-back converters can be paralleled to handle the increased power, as indicated in Fig. 8(b), to retain the advantage of the low-voltage power electronics. Medium-voltage power electronics that can withstand higher input and output voltages will be necessary when the power rating is further increased; otherwise, the cable and connector will be too weighty to handle the current. Cascaded H-bridge (CHB) and modular multilevel converters (MMCs) are discussed in the literature for offshore wind turbines [24]. Neutral point clamped (NPC) converters, illustrated in Fig. 8(c), however, will be much more feasible since they are a more compact and cost-effective solution when the voltage level is around 5 kV, whereas CHB-based converters and MMCs are more suitable for higher-voltage applications. Note that, although not shown in the figure, doubly fed induction generators (Type 3) with partially load power converters have been used in some offshore wind turbines when the power electronics were still costly. Recently installed offshore wind turbines have switched to full-scale power conversion (Type 4) for their enhanced grid fault ride-through capability, and this development is also driven by the cost reduction of power electronics. This paper focuses on Type 4 wind turbines since they are the mainstream offshore wind turbines now and will be in the future. The reconfiguration in the converter topology is mainly to handle the increasing power and voltage levels. Regarding the converter control for grid integration, Type 3 and Type 4 are not different from each other. More details are elaborated as follows.

A. OVERALL CONTROL STRATEGIES OF WTGS AND WIND POWER PLANTS

OWPP grid integration control can be generally classified into two strategies: the WTG level and the wind power plant level, as shown in Fig. 9 with a Type 4 WTG as an example. The WTG control includes the most fundamental control strategies that determine whether the OWPP fulfills the most key requirements of grid codes and the stability of the OWPP, and therefore it has a faster control response to handle FRT, current injection, and even recently harmonic mitigation, to name a few. Meanwhile, the power plant controller has a lower control bandwidth that regulates the active power and the reactive power at the PoC and targets the grid requirements of frequency and voltage regulation. The reference signals, P_{ref_WTG} and Q_{ref_WTG} , sent by the power plant controller to the WTGs should be incorporated with the WTG-level local active power and reactive power regulation to commonly regulate the wind power plant's total output power. For example, in normal operation, a WTG would generate the maximum available power based on its maximum power point tracking (MPPT); however, when the frequency controller is enabled in the power plant controller and it detects an overfrequency or underfrequency event, to comply with the grid frequency regulation, the power reference, P_{ref_WTG} , will be sent to the WTG to limit/curtail the power. Based on the minimum value

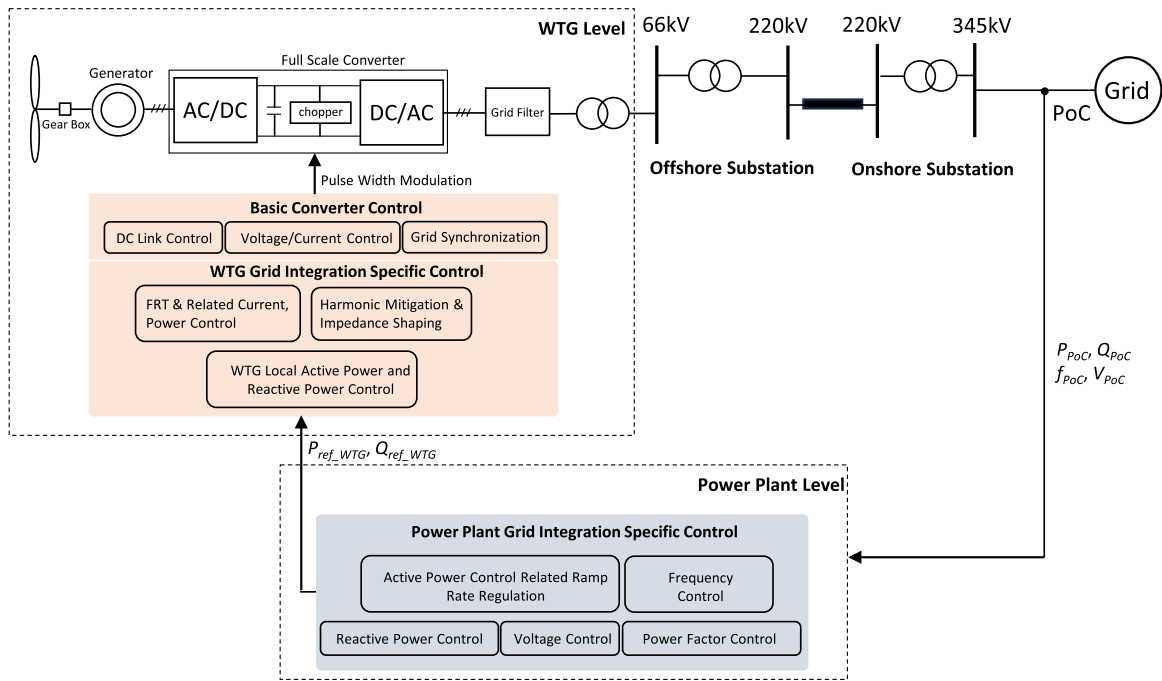


FIGURE 9. Control strategies of wind turbine plants.

driven by comparing $P_{ref,WTG}$ with the local available power, the WTG converter control regulates the output power. In an ideal case, the individual WTGs in an OWPP can directly receive external control commands like in some of the small-scale onshore applications, allowing the grid requirements to be achieved in a decentralized way without requiring investment in a power plant controller; however, this means that the f-P and V-Q at the PoC are regulated based on an open-loop control structure. The power plant-level controller is therefore preferred in a modern OWPP to achieve an accurate closed-loop regulation at the PoC to comply with grid codes. The literature review of the WTG-level and wind power plant-level control strategies is summarized as follows.

At the WTG level, many papers have been published discussing the converter control strategies, e.g., [25], [26], [27]. They are relatively mature technologies used in modern WTG systems. In addition, specifically with respect to grid integration, [28] and [29] discuss flexible active power and reactive power control based on fast current regulation during grid faults. The authors of [30] present a direct power control for a Type 3 WTG. The method controls voltage vectors based on the power errors and stator flux position with hysteresis control. It only requires stator resistance information, which improves its robustness against parameter variations. References [31] and [32] present the positive- and negative-sequence current support of WTG systems during asymmetrical faults. A review of FRT control strategies that summarizes the power injection characteristic, voltage support, and peak converter current limitation is given in [33]. In terms of harmonic mitigation, a more comprehensive discussion of harmonics will be presented in Section V of this paper.

At the wind power plant level, frequency control based on conventional droop control and spinning reserve regulation that targets grid code compliance (e.g., EirGrid) is explored in [34], whereas [35] discusses fast frequency response and presents the potential inertia response provided by frequency and active power control of OWPPs. For total wind power plant reactive power regulation, an overview of reactive power and voltage control of OWPPs is given in [36], with depictions of three fundamental reactive power control modes required by grid codes. In [37], an interesting variable-droop voltage controller for wind power plants is proposed. It considers the reactive power capacity of each WTG when automatically selecting the voltage droop gains to mitigate the PoC voltage fluctuation. Reference [38] proposes a model predictive control-based voltage control to enhance the voltage regulation and minimize the system loss in voltage source converter (VSC)-HVDC-connected wind power plants. Considering the effect of WTG active power, it can smoothen the voltage and reactive power profile of individual generators. In [39], a two-stage control scheme is proposed to mitigate the DC-link overvoltage during a fault and to facilitate the recovery. Through the DC voltage recovery trajectory designed using an adaptive voltage rise control, uninterrupted WTG operation can be achieved.

B. GRID-FOLLOWING AND GRID-FORMING CONTROL OF WTGS

Inverter-based resources (IBRs) can be divided into two categories based on their control characteristics: GFL and GFM. GFL inverters, in general, synchronize their internal reference to the grid voltage using a phase-locked loop (PLL) [40].

While remaining synchronized, they inject power into the grid, e.g., controlled by a DC-link voltage controller of the grid-side converter in a WTG, balancing the power input from the turbine (e.g., rotor-side converter injecting the maximum power) and output to the grid. As a result, they require a stiff voltage source to warrant stable operation. GFL control is common in wind turbine power plants and other variable generations because legacy power grids have been maintained with synchronous generators as the foundation to form a stiff grid upon which GFL resources can rely [41].

As the deployment of renewable generation is rapidly increasing in power systems across the globe, GFM control has been given attention [42], and it is expected to stabilize the grid in the absence or low level of synchronous generators. GFM inverters control their terminal voltage and frequency. Because they can operate without a voltage source, e.g., formed by synchronous generators, to maintain a grid, they are considered essential to stabilize future power grids with high integration levels of IBRs [43]. Based on their voltage control strategy, so-called primary control, GFM control methods can be largely classified into four different types: i) droop control [44], ii) virtual synchronous machine to mimic the machine dynamic behavior [45], iii) nonlinear virtual oscillator control to achieve improved dynamic behavior over the droop control [46], and iv) matching control [47].

Though GFM control methods feature different dynamics, especially in small timescales, they share common steady-state features, including droop characteristics, that are critical to achieving compatibility with legacy assets and power sharing among generators [48]. GFM resources can provide additional functionalities by having supplementary controls that modulate inverter dynamics under certain conditions, such as synthetic inertia to mimic the inertial response of synchronous machines [49] or virtual impedance to improve voltage regulation or stabilization [50]. These are further discussed in Section IV.

Similar to other IBRs connected to a power system, wind turbines can be controlled as either GFL or GFM sources if they are equipped with power electronics inverters to control the power flow, i.e., Type 3 or Type 4 turbines. The control type conversion requires minimum or no hardware modification because the inverter control behavior can be mostly determined by the control software. It indicates that inverters can have a mode transition during operation, e.g., between island and grid-connected modes, which is likely useful for flexible operation and resilience. Hardware redesign might be needed, however, to improve certain aspects, such as increased fault current capability for protection [51].

GFM control for OWPPs is under active research and demonstration. It is motivated by the unique aspects of offshore wind, such as long distances from the onshore grid causing a weak grid condition that makes it prone to oscillation and instability. Using GFM control, it is expected that OWPPs can stabilize the grid while being far from the grid by forming a reliable voltage profile and mitigating oscillations [52]. The active exploration of using GFM for offshore

wind is also attributed to their potential to provide grid services to enhance their value proposition, such as bottom-up black start to recover a local grid for resilience and support for bulk power system restoration, which are discussed in detail in Section IV.

As the deployment of IBRs increase, already exceeding 100% in some areas, it would be instrumental to engineer reliable inverter control methods to stabilize inverter-heavy grids. GFM control for offshore wind would be beneficial for grid stabilization and grid resilience enhancement by allowing the wind power plants to have more active and dynamic roles in power system operations. The technical merits of and trade-offs between GFL and GFM inverters, however, should be clearly understood and thoroughly evaluated through research, development, and field demonstrations, including power curtailment for GFM control by controlling the blade pitch, revenue for ancillary services, and potential systematic solutions to overcome disadvantages in a control scheme.

IV. ANCILLARY SERVICES FROM WIND POWER PLANTS

When equipped with proper control coordination and hardware design, IBRs can provide a variety of ancillary services to contribute to reliably operating a power system and/or to shorten the time of return on investment through increased and diversified revenue. Some services provide support that are inherent in synchronous machines, such as inertial response, and some services are additional, such as service restoration. Fig. 10 provides a graphical overview of the ancillary services that wind power plants can provide in different timescales overlaid with other dynamics. In the following, we discuss a few ancillary services that offshore winds have the potential to provide.

A. PRIMARY AND SECONDARY FREQUENCY RESPONSE

Primary frequency response is used to balance instantaneous supply and demand, reacting to imbalances within a few seconds in a legacy grid, which is critical to stabilize the grid. Not all generators need to provide primary frequency response (e.g., baseline generators such as nuclear power plants do not.), but a fraction should do to limit the system frequency deviation from the nominal against an imbalance. Droop control is ubiquitously used in modern power systems for this purpose, allowing multiple generators to collectively sustain a change. Droop control can also be used in IBRs, including wind power plants [44]. Programming a droop characteristic in a storage device such as a battery is straightforward [51], but it can reduce cost-effectiveness when it is applied in variable generation because it requires curtailment or additional control coordination, discussed later. To mitigate the revenue reduction due to the forgiven energy, renewable energy plants can have a deadband in the droop to prevent overreaction within a certain frequency band or to harmonize the generators' responses with different control priorities [53], which is widely accepted today.

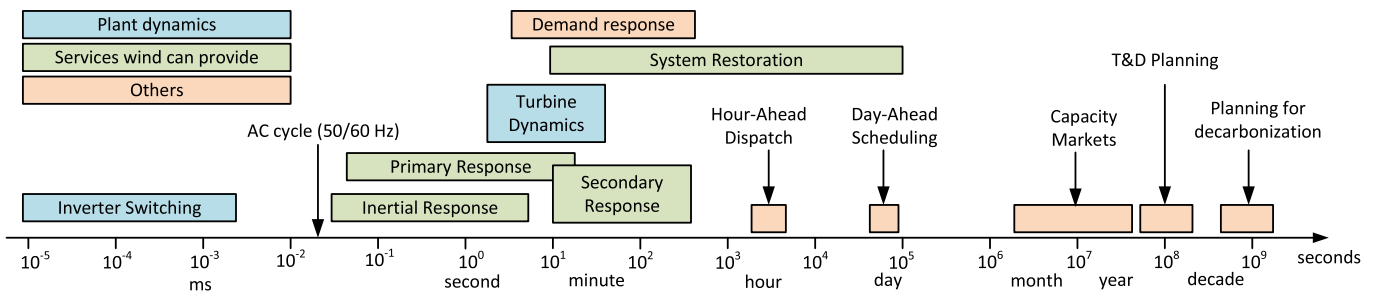


FIGURE 10. Ancillary services that wind power plants can provide in different timescales (green) overlaid with inverter and turbine dynamics (blue) and other grid components (orange).

After a generation and load imbalance, automatic generation control (AGC) recovers the system frequency to the nominal value by automatically dispatching a new asset(s) that has been reserved and/or updating generator set points. Similar to the primary response, variable generation, including wind turbines, can provide the secondary response with headroom or curtailment [54]. For the primary and secondary response, GFM control is not required in a legacy grid, but it can be beneficial in stabilizing an inverter-heavy grid over GFL control [43].

B. INERTIAL AND FAST FREQUENCY RESPONSE

The availability of a natural inertial response of a wind turbine depends on the generator type and power electronics control. Type 1 wind turbines that are directly connected to the grid can provide a natural inertial response because the turbine rotor is directly coupled to the grid [55]. On the other hand, a natural inertial response is limited in Type 3 wind turbines and unavailable in Type 4 turbines because the power electronics converters decouple the turbine and the grid.

Synthetic inertia has been studied to explore solutions to compensate for the decreasing inertia in the modern grid [56]. It has been demonstrated that Type 3 and Type 4 turbines can emulate the inertial response of synchronous machines, and therefore this is called synthetic inertia. By exploiting the hidden inertia in the rotor, a wind turbine can provide inertial response. As shown in [57], the emulated inertia is programmable by control parameters. The amount of inertial response realizable, however, depends on the inverter operating point due to the inverter current limit, which is a distinguishing aspect from the natural rotational inertia [49]. For instance, if the current reference commanded to fully emulate the synthetic inertia exceeds the current limit, the inertial response would be saturated to the limit. To relieve the hard limit, inverters can be oversized or designed to sustain a momentary overcurrent, which can also be used to improve other ancillary services, including black start to sustain a higher inrush current and fault current to facilitate system protection [51].

Synthetic inertia can be realized in different ways. For VSC-HVDC-interfaced OWPPs, it is not straightforward to

involve the wind turbines with the onshore grid for the inertial response because they are not synchronous. In this case, synthetic inertia can be realized by feeding the onshore grid frequency deviation to the offshore wind power plants through communications [58]. Further, to improve the response, the energy stored in the HVDC link can also be used for the synthetic inertial response without a significant delay.

The synthetic inertia can be defined as a subset of fast frequency response that includes responses to counteract a frequency change [59]. Both synthetic inertial and other fast frequency responses would be beneficial for improving the frequency nadir by promptly providing the deficient power. On the other hand, because it emulates the voltage source behavior of a machine, by slowing down the rotational frequency change, i.e., a virtual synchronous machine type of GFM, the synthetic inertial response could outperform other types of fast frequency response without an inertial mechanism suppressing the RoCoF [59]; however, more study should be done to explore novel approaches that can excel in zero-inertia grids.

C. BLACK START

A black start is a critical step in power system restoration to establish a grid after a blackout using a generator that can start without having an external voltage already formed. It requires a generator designed to sustain significant transients occurring during the process, providing a reliable voltage source to energize critical loads and a cranking path for the other generators. Because black starts have been exclusively provided by synchronous generators, such as hydropower or thermal power plants [60], concerns about reliance on the machines and thus system resilience in inverter-heavy grid scenarios, along with increasing natural disasters causing frequent power outages, have been raised. The transformational change naturally motivates studying the technical feasibility of inverter-driven black starts [61]. Embedding black-start capability in OWPPs has brought significant attention due to its potential to enhance the OWPPs' self-survivability during blackouts and grid resilience. Being able to form a local grid based on offshore wind would not only unlock the path for extreme grid resilience but also facilitate bulk power system restoration, i.e., a bottom-up approach.

The concept of the inverter black start poses technical challenges resulting from the fundamental differences between power electronics inverters and synchronous machines. First, the inverter's limited short-circuit current (in general, 1.1 p.u.–1.5 p.u. compared to 6 p.u.–8 p.u. of synchronous machines) should be given careful attention because it affects system behavior under transformer energization or motor startup, which causes a heavy inrush current, potentially exceeding the inverter rating [62]. On the other hand, soft-start techniques, such as inverter voltage ramp-up, can suppress the inrush current during the initial energization, though the black-starting inverters could encounter a significant inrush as they sequentially energize segments of a grid, such as an HVAC step-up transformer, until they obtain enough total generation capacity [63].

In a multiple inverter-driven black start, e.g., an offshore wind power plant where a large number of wind turbines are involved in the task, parallel inverter operation is critical. Leader-follower coordination requiring reliable communications can degrade the robustness of the black start and/or might not be economic or feasible in case the generators are distant, such as in the case of OWPPs, so reliance on communications should be avoided or minimized. Involving multiple inverters in a decentralized manner would be beneficial to resolve these issues and for system resilience, avoiding the single point of failure [64].

Deploying a black-start service using an OWPP, which is not yet used in today's grid operations, would require significant efforts in research, development, and demonstration at scale together with grid code updates based on consensus among stakeholders. To elucidate the pathways, the following summarizes the state of the art of these technologies found in the literature.

Black start using a 1.2-MW Type 3 wind turbine for a low-voltage island and resynchronization has been simulated in [65]. The configuration adds storage in the DC link of the turbine inverter to form a local grid. The system's operation is similar to a DC-coupled photovoltaic system with a battery; it allows for retaining the MPPT operation of the variable generation with power flow injected into the DC link decoupled from the grid, thus mitigating its intermittency at the cost of added complexity. An AC-coupled configuration is also possible, such as using synchronous generators (like diesel generators) or operating GFM inverters to form the grid in parallel with wind turbines and to kick-start the OWPP, keeping the wind turbines' grid-side converter in GFL mode with MPPT or a normal (non-black-start-capable) GFM mode. This configuration, however, might not be preferred or economic because the system performance and reliability depend on the supplementary device, exposing the single point of failure. To unlock the full potential of the offshore wind, built-in black-start and GFM capability in the wind turbine should be pursued.

Reference [66] simulated a black start using multiple wind turbine synchronization in a 1-GW offshore wind power plant using a distributed PLL-based frequency control, a type of

GFM. Notably, the method uses a frequency-reactive power droop, the opposite of the conventional droop, $\omega - P$, to improve the reactive power sharing among turbines without inter-turbine power circulation. It is beneficial because the reactive loading is dominant during the initial black-start process resulting from submarine lines and transformers that vary from one turbine to another. This work details the system dynamics of a sequential black start by including the inverter filter and grid-interface transformer dynamics and turbine-by-turbine energization using breakers, which demonstrates the potential challenges and solutions in the inverter-driven restoration process. Following the dynamic recombination of the GFM wind turbines, they sequentially energize the grid, including the HVDC lines and the VSC-HVDC-based, on-shore load. It assumes individual wind turbines are equipped with a small local storage to self-start, such as uninterruptible power supply, which is common in wind turbines. Similar to other works, [66] assumes well-regulated DC-link voltage; it does not model generator side dynamics, which would be necessary to fully confirm the technical feasibility of offshore wind for black-start service, followed by hardware demonstrations in the field.

As discussed, offshore wind is promising to provide multiple ancillary services to meet the needs in future grids with large amounts of renewable generation. Because they require additional controls superimposed on the primary turbine control and also likely plant-level control, however, the dynamic interactions among different function blocks should be analyzed, and they should be harmonized to collectively maintain the grid in parallel with other assets. Table 5 summarizes this discussion with key takeaways.

V. HARMONICS

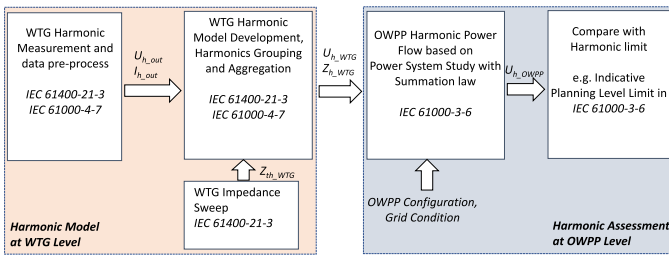
Harmonics is another crucial topic regarding the grid integration of offshore wind power plants [67]. The harmonic requirements for OWPPs have been elaborated in Section II E. This section further discusses the industry practice on how to perform harmonic studies and evaluate whether OWPP emissions meet the requirements.

A. HARMONIC PROPAGATION

In industry practice, usually only the harmonic voltage limit at the PoC (sometimes the busbar inside the wind power plant) is provided by the wind power plant developer to the wind turbine manufacturer. The harmonic level at the PoC is a joint effect of the emissions of each wind turbine in the OWPP and the grid background noise; however, they are not simply added up at the PoC because the cable impedance and the grid impedance affect the harmonic propagation. To properly consider the propagation, a harmonic model of the wind power plant needs to be built up, and a harmonic study of the OWPP needs to be performed. The OWPP harmonic assessment procedure using a WTG harmonic model with relevant IEC standards in each step is shown in Fig. 11. The harmonic model of the WTG should be presented in a frequency domain among various power bins, and hence the aggregation

TABLE 5. Overview of Ancillary Services Available From Wind Power Plants.

Service Type	Description	Availability in WTG
Primary frequency response	Balances instantaneous supply and demand by reacting to imbalances within a few seconds. Critical to stabilize the grid.	Available but requires curtailment or additional control coordination, which could reduce the revenue from energy generation but can be monetized for the service.
Secondary frequency response, frequency recovery through dispatch coordination with AGC	Contributes to recovering the system frequency to the nominal value with set point dispatch.	Available by updating the power set points of wind turbines but could yield suboptimal energy generation from wind power plants at the cost of ancillary service provision. The degree of involvement of wind power plants for this would be a trade-off between the grid service and the energy generation.
Inertial response, a subset of fast frequency response	Suppresses a frequency change against an imbalance of supply and demand. Synchronous generators provide rotational inertia through their electromechanical coupling with the prime mover.	Depends on the generator type and power electronics control. Natural inertial response is limited in Type 3 or unavailable in Type 4 due to decoupling. Synthetic inertia is available by power electronics control reacting to a system frequency change. Amount of synthetic inertia realizable depends on inverter operating point.
Black start, system restoration	Establishes a grid from a blackout. Synchronous generators have served as black start resources with fuel/storage reserved for restoration.	Embedding black-start capability in OWPPs would unlock the path to extreme grid resilience and facilitate bulk power system restoration.


FIGURE 11. OWPP harmonic evaluation procedure.

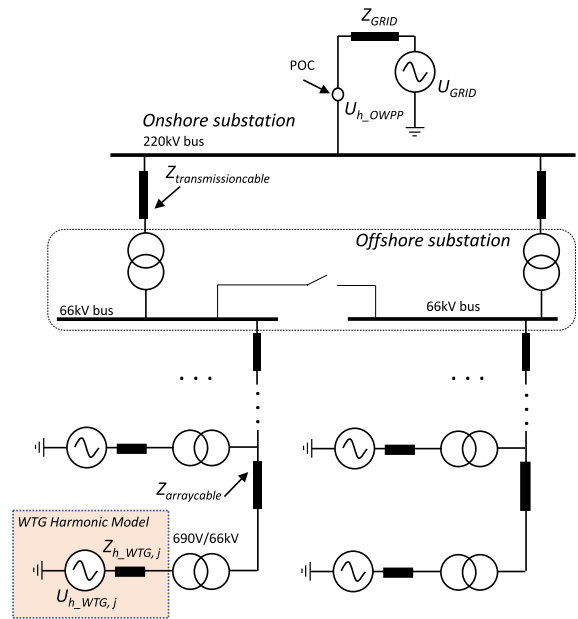
according to IEC 61400-21-1 [18] and spectral component grouping according to IEC 61000-4-7 [68] is needed. After obtaining the harmonic model of a single WTG, the power system study with harmonic power flow can be executed to study the total harmonic emissions of the OWPP. Note that the harmonic, U_{h_WTG} , is a phasor value, with a magnitude and angle, and the randomness of the phase angles of individual WTGs should be included in the model in the summation process.

A more detailed illustration of how the effect of each WTG's emissions is aggregated at the PoC is shown in Fig. 12. In the model, there are $n+1$ independent sources, including n harmonic voltage sources representing WTGs, and one depicting the grid background noise. In the so-called harmonic power flow, each time only one source is considered (others are assumed to be zero). For instance, to evaluate the impact of the WTG j on the harmonic level at the PoC, only $U_{h_WTG,j}$ keeps its value, and the other sources are assumed to be zero. Then, after running a harmonic power flow, an emission, $U_{h_OWPP,j}$, will be obtained at the PoC. The total emissions of the OWPP at the PoC are calculated according to the summation law as defined in IEC 61000-3-6 [20]:

$$U_{OWPP} = \sqrt{\sum_{j=1}^n U_{h_WTG,j}^{\alpha}} \quad (4)$$

where indicative values of α are shown in Table 6.

If the phase angles of $U_{h_WTG,j}$ are quite certain (usually for low-frequency harmonics), the $\alpha = 1$ can be applied no matter the frequency order. Note that the model shown in Fig. 12 should include all the components in the OWPP as


FIGURE 12. Example model for the harmonic study of OWPPs.
TABLE 6. Indicative Summation Exponents for Harmonics in IEC 61000-3-6:2008

Harmonic order	α
$h < 5$	1
$5 \leq h \leq 10$	1.4
$h > 10$	2

long as it has an influence on the harmonic level at the PoC, e.g., a filter, a STATCOM. The PoC is not a technical definition but an agreement of liability between the wind power plant developer and the grid operator, so it might be another node instead of the one shown in Fig. 12. Because an OWPP may need to be reconfigured in case of a component failure in the system, the harmonic study needs to be done in all possible cases.

B. HARMONIC MITIGATION

Mitigation measures must be taken if the harmonic emissions of the OWPP exceed the limit at the PoC. A straightforward

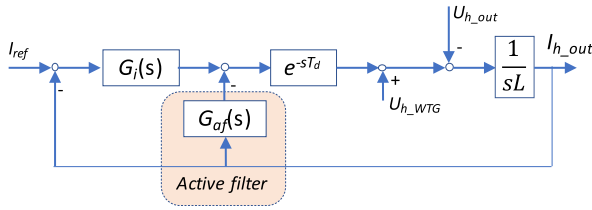


FIGURE 13. Diagram of the grid-side wind power converter control with an active filter.

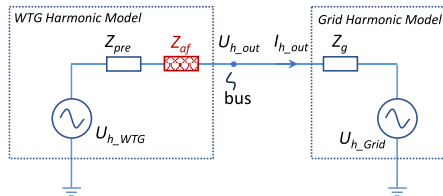


FIGURE 14. WTG harmonic model with an active filter.

way is to put a band-pass or high-pass passive filter at or near the PoC [69] to provide a low-impedance path for the harmonics and thereby mitigate them. In OWPPs, however, the passive filter can only be put in either the nacelle of the wind turbine or the offshore platform, both of which have a high cost per square meter. Further, [70] shows that the harmonic issues in the bandwidth of the converter controller are usually matters of impedance matching, while an active power filter (APF) does not necessarily achieve impedance matching. Alternatively, an active filter (also named virtual impedance), if tuned properly, can achieve impedance matching, and it also introduces flexibility, which means that the filter can still be tuned after deployment if the configuration of the OWPP changes and thereby the harmonic issue changes [71], [72].

An example application of active filters is shown in Fig. 13, where only the current control loop is considered because the harmonic issue usually happens in the bandwidth of the current control loop. In the figure, I_{ref} is the reference of the current control. $G_i(s)$ is a compensator. e^{-sT_d} is the total delay caused by the control and the Pulse Width Modulation (PWM) converter. L is the power filter of the WTG. $G_{af}(s)$ is the active filter. The impedance model of the WTG is derived in (5) and shown in Fig. 14, where $Z_{pre}(s)$ is the impedance of the WTG without active filters, and $Z_{af}(s)$ is the extra impedance introduced by the active filter.

$$Z_{WTG} = \underbrace{sL + e^{-sT_d} G_i(s)}_{Z_{pre}(s)} + \underbrace{e^{-sT_d} G_{af}(s)}_{Z_{af}(s)}. \quad (5)$$

The voltage harmonic distortion on the 66-kV bus (in some OWPP, there are 33-kV buses instead), as shown in Fig. 12, usually has to fulfil an upper limit and, therefore, needs to be checked by harmonic study. According to the harmonic model depicted in Fig. 14, the harmonic voltage on the bus can be expressed by (6). It shows that the bus voltage distortion can be affected by the active filter or virtual impedance, Z_{af} .

It is not straightforward to derive the design of the virtual impedance from (6) to reduce the bus voltage distortion. In fact, the typical reason for harmonic voltage issues on the bus is that the WTG impedance $Z_{pre}(s)$ and the grid impedance $Z_g(s)$ together form an LC resonant circuit with underdamping. Thereby, the denominator of (6) without the active filter $Z_{af}(s)$ will be close to zero and induces a peak voltage U_{h_bus} at the resonant frequency. It can be effectively mitigated by adding a resistive virtual impedance at the harmonic or resonant frequency. This approach has been demonstrated and verified in an offshore wind power plant, and the details are reported in [73].

$$U_{h_bus} = U_{h_out} = \frac{U_{h_WTG} Z_g - U_{h_Grid} (Z_{pre} + Z_{af})}{Z_{pre} + Z_{af} + Z_g}. \quad (6)$$

VI. WIND POWER PLANT STABILITY ANALYSIS

Ideally, the stability analysis of an OWPP should use the detailed OWPP model and check the stability in all operating conditions, but this approach is usually not feasible due to the huge amount of calculations; thus, a crucial matter in stability analysis is model simplification. A typical approach is to first perform a small-signal model based stability analysis. Once any stability issues are observed, a detailed model-based electromagnetic transient (EMT) simulation is carried out to verify the stability issues.

A. SMALL-SIGNAL STABILITY

State-space models are usually used for stability analysis at the system level. Compared with other black box models (transfer functions), state-space models also consider the states inside the system, which reduces the errors in the stability analysis. Nonetheless, the computational effort can make the analysis unfeasible when considering the state space of all the WTGs in an OWPP. To solve this, aggregation is usually needed in building the state-space model of the OWPP. Another often-mentioned drawback of the state-space model is its low scalability [74]. On the contrary, in impedance modeling, each component—including cables, transformers, and WTGs—has an independent model, which makes scaling the model much easier. Moreover, impedance modeling considers only the relation between the input and output of a system, which, although it overlooks some dynamics inside the system, simplifies the modeling and reduces the computational cost, especially for a large system stability analysis.

Nonetheless, the impedance model of a wind turbine is more complicated than the cables (purely passive), and it is influenced by both the control and power components of the wind power converter (grid side). There are two categories of impedance modeling of the wind power converter. One is frequency scan based, where a detailed simulation model of the wind power converter is needed. By injecting a voltage perturbation from the grid side to the wind power converter, a current perturbation can be obtained in the grid current. The ratio between them is the impedance, which is, of course, frequency dependent. The frequency scan-based impedance

model is simple and effective, but it can be limited by measurement errors. There are also analytical impedance models, which are formulas with design parameters including control and hardware as inputs. To build an analytical impedance model, the wind power converter needs to be linearized; however, the wind power converter, especially the control, is highly nonlinear. In past years, the effort on analytical impedance modeling was mainly to take into account the nonlinearity of the converter step by step, including the PLL, the frequency coupling, the imbalance, etc. [75], [76]. Various small-signal modeling approaches of inverters for stability studies are reviewed in [74].

Impedance-based stability analysis has limitations because it analyzes the stability of only one connection point at a time. Therefore, although the analysis can estimate stable operation at a connection point, it can reveal instability at a different point. This can be misleading because in this case the system is unstable. To avoid this misunderstanding, when performing an impedance-based stability analysis of a wind power plant, the study must evaluate the stability of all buses.

B. LARGE-SIGNAL STABILITY

The small-signal model-based stability analysis is only valid when the system is around an equilibrium point. In reality, the system can move from one equilibrium point to another due to, e.g., wind speed variation, energizing of the OWPP, the kick-in of a WTG after maintenance, or a cutoff of a cable with failure. Then, the assumption that the system has only small perturbations is no longer valid, and thereby the small-signal model-based stability analysis is no longer valid. In this case, a detailed model-based EMT simulation is usually performed to check the stability. Time domain simulation can only indicate the stability for one initial condition at a time, and it does not provide a closed-form solution to the transient stability problem. Moreover, time domain simulations with stiff differential equations can be computationally intensive [77]. To make the computational effort affordable for an EMT simulation, a string with multiple WTGs in an OWPP is sometimes aggregated to one WTG in the model, which will then increase the error of the stability analysis.

Lyapunov-based techniques provide another possibility for large-signal stability analysis. The main advantage of Lyapunov-based approaches is in the fact that a Lyapunov function allows the estimation of the region of attraction of a stable operating point instead of a single operating point (small signal-based approaches), which can help identify the acceptable size of the disturbance for stability [78]. A proper Lyapunov function is usually difficult to define, however, which makes its application limited.

VII. WIND POWER PLANT TRANSMISSION SOLUTIONS

Depending on how the OWPP is connected to the onshore substations, one can classify its transmission solutions into two approaches: HVAC and HVDC. Intensive research has been carried out to compare the trade-offs between them [79],

[80], [81]. From the design perspective, HVAC has the advantage of cost (cheaper, due to the lack of converter stations) and schedule (shorter, typically 3–4 years) compared with HVDC (typically 5–6 years) for distances to shore between 80–100 km. The typical tipping point from a cost perspective between HVAC and HVDC is around 120 km, where the HVAC mid-point compensation is considered; however, HVAC technology is more dependent on the stiffness of the power grid. It requires a system integration approach for the primary equipment selection and integrated system design studies (e.g., reactive power compensation, steady-state harmonics, and stability), whereas HVDC is typically a point-to-point approach with one original equipment manufacturer handling both interfaces at offshore (between the offshore converter station and the WTG) and onshore (between the onshore converter station and the power grid). The HVAC-connected OWPP is traditional and still massively applied in ongoing projects due to its advantage of low station cost, for example, in Hornsea I and Hornsea II [82]. Some recent research indicates that HVAC configurations could be reconsidered for long-distance OWPP applications, including mid-cable reactive power compensation and newly developed AC cables of higher voltage ratings [83], [84]. Another alternative approach to increase the HVAC transmission capacity is to use a relatively low frequency or fractional frequency that reduces the skin effect in the conductors [85], [86], though it brings disadvantages such as additional investment in the onshore converter station.

HVDC has risen in recent years as the most viable technology to transfer power from large OWPPs to onshore grids over distances of more than 100 km mainly due to the significantly lower transmission losses. The 400-MW BorWin1 plant is the first OWPP that is connected to the power grid using HVDC technology—at ± 150 kV over a transmission distance of 200 km [87]. The 3.6-GW Dogger Bank A, B, and C schemes, which will be connected to onshore grids through three 1.2-GW HVDC connections, and 2.852-GW Hornsea 3, which will be connected with two 320-kV HVDC connections, are the largest offshore wind power plants currently under construction [88], [89]. Although all HVDC systems installed or currently under construction to connect OWPPs are based on the VSC technology using point-to-point links, significant research and development have been carried out to explore other design options. The following discusses different system and converter configurations and outlines the main control and operational challenges for HVDC-connected OWPPs.

A. HVDC CONVERTER TECHNOLOGY AND SYSTEM STRUCTURE FOR OWPP GRID INTEGRATION

1) VSC-HVDC SYSTEMS

The main features of VSC-HVDC systems using MMCs [90] include modular design, high-quality AC voltage generation, low power loss, independent control of active and reactive power, and the capability of establishing an AC network.

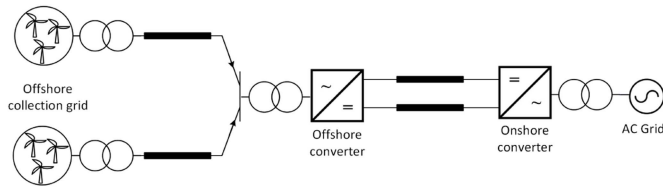


FIGURE 15. Typical point-to-point HVDC link for OWPP connection.

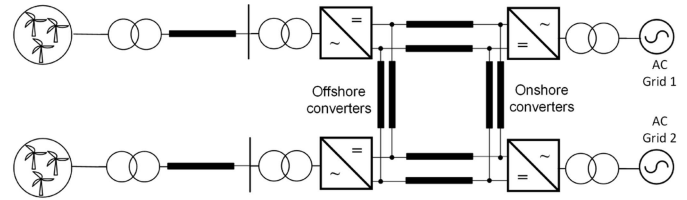


FIGURE 17. Four-terminal MTDC system for connecting two large OWPPs.

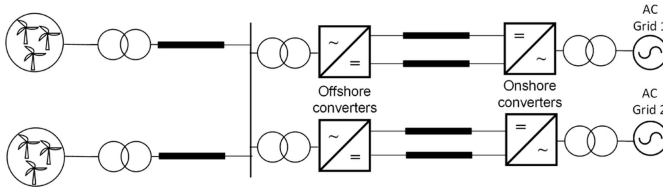


FIGURE 16. Parallel connection of HVDC links for OWPP connection.

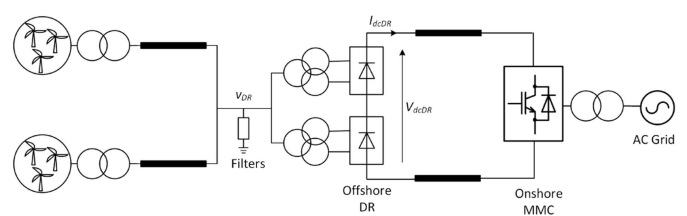


FIGURE 18. Configuration of using DR-HVDC for connecting large OWPPs.

These features make VSC-HVDC more attractive for connecting OWPPs than other HVDC technologies. Different systems have been proposed and studied.

a) *Point-to-point systems*: Point-to-point HVDC systems, as shown in Fig. 15, have the simplest structure. They consist of an offshore rectifier station, which establishes the OWPP AC network and converts the offshore AC power into DC, and an onshore inverter, which converts the DC power back to AC to be exported to the onshore AC network.

b) *Parallel configurations*: For a large OWPP that requires multiple converters, a parallel connection of the OWPP, as illustrated in Fig. 16, can be adopted [91], [92]. In this configuration, the OWPP is connected to the offshore AC collectors through AC cables and transformers, and two parallel HVDC links are used to transmit the generated wind power to the onshore sites. With this configuration, the availability of the system can be improved. For example, when one HVDC link is out of service due to faults, the majority of the generated power can still be exported to the onshore grid through the other link [4]. In such a parallel arrangement, extra controls need to be allocated to the offshore HVDC stations to allow proper power sharing [91], [92].

c) *Multiterminal HVDC configurations*: Significant research and development on the use of a multiterminal HVDC (MTDC) network for connecting multiple OWPPs to different onshore network connection points has been carried out [93], [94]. In 1988, the Sardinia-Mainland Italy HVDC link, 200 MW at 200 kV, added a third converter station, rated at 50 MW, at Lucciana on Corsica to allow flexible power flow, forming the first MTDC system [95]. The new converter station used thyristor valves instead of mercury-arc valves, which had been used for the other stations; they were replaced with thyristor-based technology in 1992. A VSC-HVDC technology-based MTDC system was developed in 2013 in Nan'ao, China [96]. The three-terminal pilot project with transmission capacities of 200 MW/100 MW/50 MW at ± 160 kV interconnects the wind power plants in Nan'ao

Island to the onshore grid. In 2014, a five-terminal MTDC system was commissioned in Zhoushan, China, with converters rated at 400 MW/ 300 MW/ and 100 MW with a transmission DC voltage of ± 200 kV [97]. The most notable MTDC installation so far is the 4-terminal ± 500 -kV Zhangbei MTDC system commissioned in 2019 [98]. It has two converters rated at 3000 MW, and the other two are rated at 1500 MW. In Europe, the first three-terminal MTDC system using VSC-HVDC technology will be commissioned in 2024 in the United Kingdom [99]; it is rated at ± 320 kV and contains three stations rated at 1,200 MW/ 800 MW/ and 600 MW, respectively. Fig. 17 illustrates a four-terminal, meshed MTDC network connecting two large OWPPs. Various studies have shown that MTDC links improve power exchange flexibility between multiple areas and provide better system redundancy [100], [101]. To ensure stable operation and proper power sharing, coordinated controls—such as droop control and leader/follower control—have been investigated in the literature [102], [103], [104].

2) DR-HVDC CONFIGURATIONS

A diode rectifier (DR)-based HVDC is another potentially promising topology for OWPP integration [105], [106]. As illustrated in Fig. 18, in this configuration, the offshore station uses a number of DRs connected in series on the DC side and in parallel on the AC side of the OWPP network. Offshore capacitor filter banks are also connected to provide reactive power compensation and harmonic filtering. An MMC-based, onshore converter is used to convert the DC power to the onshore AC grid. Compared with the VSC-HVDC transmission system, DR-HVDC has the potential benefits of reduced offshore station volume and weight, higher conversion efficiency, and shorter plant delivery time, thus leading to a lower overall investment. For example, it has been shown that compared with VSC-HVDC connections for offshore wind power plants, the volume and transmission losses can be reduced by 30%

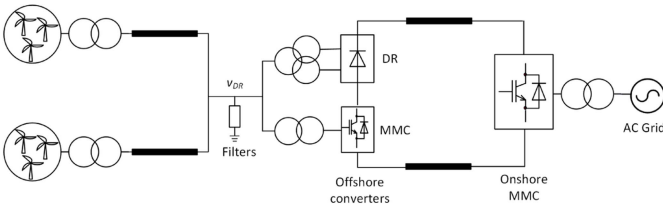


FIGURE 19. Configuration of series-connected DR-HVDC and VSC-based HVDC.

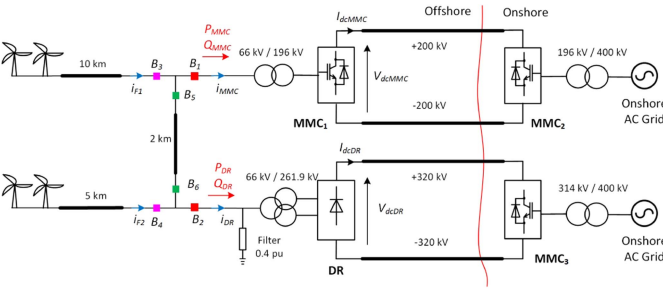


FIGURE 20. Hybrid converter station of parallel-connected DR-HVDC and MMC-HVDC systems [92].

and 20%, respectively, and the total cost can be potentially reduced by 30% [107], [108]. DRs, however, cannot establish the offshore power network like the MMC counterpart does, and therefore WTGs must perform frequency and voltage control for the offshore collection AC network. Starting up the offshore system is also a challenge due to the unidirectional power flow of the DR-HVDC system. Having GFM control capability in WTGs could benefit this configuration.

3) HYBRID CONFIGURATIONS

i) Hybrid configurations for offshore converters: The series connection of different converter configurations on the DC side for the offshore station has been considered to take advantage of different technologies. For example, [109] investigates the operation of a series-connected, line-commutated converter and VSC, whereas [110], [111] study the series connection of a DR and VSC/MMC, as shown in Fig. 19. The offshore MMC establishes the offshore AC voltage while it also regulates the DC voltage of the HVDC link by controlling the active power exchange between its AC and DC sides. Moreover, the offshore VSC can also be controlled to operate as an active filter for the 11th- and 13th-order harmonic currents to reduce the requirement for the passive filters needed by the DR [110]. Under this arrangement, offshore WTGs can be implemented similar to wind power plants with HVAC or VSC-HVDC connections. Harmonic suppression control of the offshore MMC is further explored in [111] to include the elimination of the 23rd- and 25th-order harmonic currents.

b) Hybrid converter stations: The parallel operation of DR-HVDC and VSC-HVDC stations for OWPP transmission is proposed in [92], as shown in Fig. 20. This application can

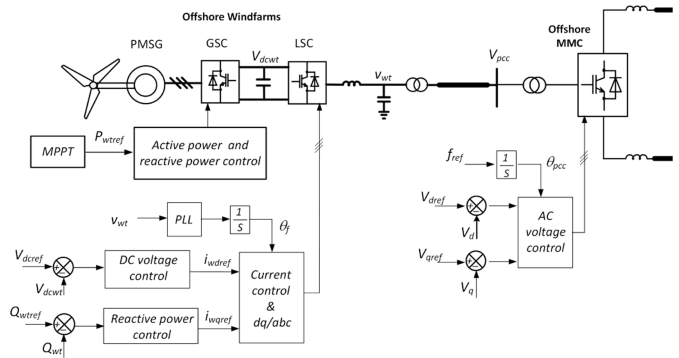


FIGURE 21. Control diagrams of WTG and VSC-HVDC for offshore wind power plant transmission.

be considered when a new OWPP is developed in an area within the vicinity of an existing OWPP that is connected to the onshore through a VSC-HVDC link [92], [112]. A new DR-HVDC link can be installed with its offshore AC side connected to the existing OWPP and VSC station, and the DR-HVDC and VSC-HVDC links operate in parallel. By connecting a DR and VSC on their AC sides, the offshore VSC station is capable of energizing the offshore grid and WTGs. It can also actively compensate reactive power and suppress harmonics generated by the DR-based station, if required, to reduce the AC filter switching during the variation of wind speed [113]. Thus, this potentially provides a promising solution to reduce the control complexity of WTGs associated with DR-HVDC systems; reduce power losses, volume, and capital cost; and increase redundancy and availability.

B. SYSTEM CONTROL STRUCTURE

1) VSC-HVDC

The operation of VSC-HVDC-connected OWPPs has been well described in [114], [115], [116], with the control scheme on the offshore side illustrated in Fig. 21. The onshore converter station regulates the DC voltage of the HVDC link according to the set point, whereas the offshore VSC station is controlled to resemble an AC voltage source to regulate the offshore AC voltage and frequency. Thus, the control strategy adopted for WTGs is the same as the AC connection, e.g., the generator-side converter controls the active power generated by the WTG, and the line-side converter controls the WTG DC voltage and reactive power. The generated wind power is automatically absorbed by the offshore HVDC converter and converted to DC power.

2) DR-HVDC

In a DR-HVDC system, similar to a VSC-HVDC system, the onshore VSC station usually regulates the DC voltage to the set point; thus, the amount of power that is transmitted through the DC system is dependent on the DC voltage at the offshore DR terminal. Considering a 12-pulse DR arrangement, the generated DC voltage is determined by the AC voltage amplitude, V_{ac_off} , DC current, I_{dc} , and AC side reactance, X ,

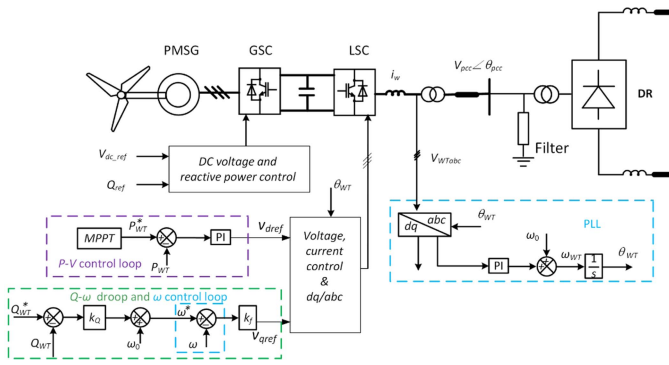


FIGURE 22. Distributed PLL control for DR-HVDC-connected OWPPs [66].

given as:

$$V_{dcr} = 2 \left(1.35V_{ac_off} - \frac{3}{\pi}XI_{dc} \right) \quad (7)$$

Thus, the active power transmitted from the OWPP to the onshore HVDC can be regulated by the magnitude of the offshore AC grid voltage V_{ac_off} .

Different control methods for DR-HVDC-based OWPPs are investigated in [66], [117], [118], [119], [120]. The authors of [117], [118] propose the control strategy based on external centralized controllers, where the WTG-level control of this solution is similar to that of the VSC-HVDC; however, an external centralized controller is required to regulate the offshore frequency and voltage at the offshore point of common coupling (PCC), which is shared with all the WTGs through communications. Thus, the system performance relies on communications, which can cause severe issues in case of a communication delay or failure. To address the communication issue, a distributed PLL-based P-V and Q-f control method is proposed in [66], as illustrated in Fig. 22. As shown, the WTG active power is controlled by regulating its terminal AC voltage amplitude, and a Q-f droop is used to ensure reactive power sharing among the different WTGs. This control method enables each WTG converter to operate as a GFM source and autonomously contribute to the overall offshore voltage and frequency regulation, providing WTGs with plug-and-play capability for easy synchronization to the offshore network.

An alternative control method, called FixReF control, is proposed in [119], [120] for DR-HVDC-connected offshore WTGs using Global Positioning Systems (GPS). In this method, the GPS is used to provide a fixed frequency reference and common angular reference for all the WTGs; thus, the remote measurements for the offshore PCC frequency and angle required in [117] can be avoided. The FixReF control solution differs from PLL-based controls because the rotating reference axis provided by the GPS no longer aligns with the voltage vector. The main drawback of this control is the reactive power sharing issue among the WTGs, and the use of the GPS also leads to reduced robustness.

C. SYSTEM CONTROL AND OPERATION DURING FAULTS

HVDC-connected OWPPs are mainly constructed with power electronics converters, which are vulnerable to overcurrent and overvoltage in case of network faults [121]. Thus, system control and protection during various faults, including offshore and onshore AC faults and DC faults, are significantly important and need to be carefully considered and designed. Due to the space limit, only AC faults are briefly reviewed here; DC faults, which are rare, are not included.

1) OFFSHORE AC FAULT

In case of an offshore AC fault, the rapid drop of offshore AC voltage could potentially lead to overcurrent of the offshore HVDC converter stations. To limit the fault current, the current-voltage droop method is proposed in [122], which adjusts the output voltage reference according to the measured offshore three-phase currents. Alternatively, the cascaded vector control with inner current loop and outer voltage loop has been proposed [123], which has the capability to limit the overcurrent during offshore AC faults. System control and operation during asymmetrical offshore AC faults is challenging for HVDC-connected OWPP operation because VSCs can exhibit undesirable performance, such as output current distortions, DC-link voltage, and output power oscillations. To tackle these issues, the double-synchronous reference frame for the control of conventional VSC systems, where the AC voltages and currents are decomposed into positive- and negative-sequence components, is commonly used [124], [125]. Various control objectives, including the suppression of negative-sequence currents (to maintain balanced AC currents) and the nullification of oscillating active power (to prevent the injection of double-line frequency oscillating power into the DC side), have been considered. Reference [126] reports that during asymmetrical faults, overvoltage can occur in nonfaulty phases, which could lead to the disconnection of the offshore WTGs. In addition, [127] highlights that simply suppressing the negative-sequence current from both the offshore MMC and WTGs to zero is inadequate. The authors propose a modified approach to control the fault currents to enable fault detection and discrimination to prevent overvoltage in the offshore network and to accelerate offshore AC voltage recovery following the clearance of AC faults.

2) ONSHORE AC FAULT

During onshore AC network faults, the power transmission capability of the onshore converters is severely reduced. The continuous power export from the OWPP to the HVDC link leads to a power imbalance and can result in rapid rising of the DC-link voltage. To avoid a shutdown of the entire system, the excess power must be dissipated or the OWPP needs to reduce the power injection. DC choppers or dynamic braking resistors connected at the onshore HVDC terminal can be used but lead to an increase in capital costs [128]. Power reduction control with the aid of a fast communication system is employed in [129], [130]. When the fault is detected by the

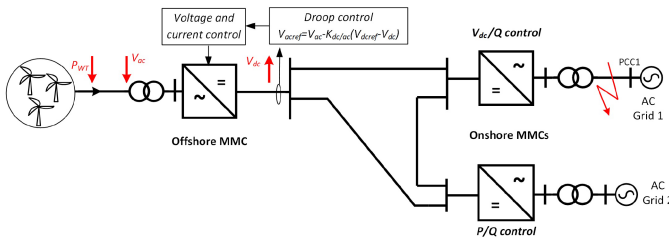


FIGURE 23. Onshore fault ride-through V_{dc} - V_{ac} droop control [131].

onshore converter, the communication system will distribute the fault signal to the WTGs to reduce the power generation. Under such arrangements, however, the system performance mainly relies on communication reliability and speed, potentially reducing the robustness of the system. Reference [131] proposes a method that uses the V DC-V AC droop control, such that the offshore MMC reduces the offshore AC voltage magnitude according to the increased DC voltage, as shown in Fig. 23. Consequently, the WTG grid-side control will reach the current limits imposed at the outer controllers, leading to the automatic power reduction of individual WTGs. This method can effectively reduce the onshore terminal power stress and improve the system reliability and robustness.

VIII. CONCLUSION

This paper presented an overview of offshore wind power grid integration from both industry and academic perspectives. Section II provided an overview of grid codes and listed key requirements regarding OWPP grid integration. In the future, there will be a more pressing need for harmonizing grid codes, like the practice of ENTSO-E, to reduce the extra burden on manufacturers to avoid excessive WTG parameterization and to realize the massive deployment of OWPPs in a timely manner. Sections III and IV reviewed WTG and wind power plant control strategies and ancillary services related to grid compliance, grid support, and resilience. The discussion elucidated the potential for offshore wind to not only overcome the grid integration challenges but also to benefit the land-based grid with breakthrough power electronics technologies, including GFM inverters, black start, and synthetic inertia, to name a few. Sections V and VI discussed harmonics and the stability analysis of OWPPs as they relate to concerns about the operation of modern power systems with high integration levels of wind generation, especially because the integration of OWPP, which is located far from the land-based grid, causes concerns in power quality. Finally, Section VII reviewed the transmission approaches for OWPPs, with an emphasis on HVDC connections that show great potential in modern, large-scale, offshore wind projects, and it discussed new approaches, such as MTDC, to facilitate OWPP deployment by exploiting the existing infrastructure of neighboring OWPPs for cost reduction and improved redundancy.

Offshore wind is expected to grow exponentially to drive decarbonization and transform the power system landscape,

which will pose challenges, so more stringent research and development across the globe will be paramount. In this paper, we discussed the outstanding challenges in these related technology areas. First, more joint efforts from utilities, developers, and manufacturers need to be enforced toward harmonizing grid codes, standards, and guidelines. Second, although utilities emphasize enhancing the flexibility of the power system, the expansion of technology enablers—such as GFM technology alongside other ancillary services with proper technical specifications as common industry guidance and proper utility and government incentives and tariffs—remains a challenge. Third, harmonics and stability issues, which are extensively investigated in academia and summarized in this paper, still require screening of the proper methods and integration of the cutting-edge analytical approaches into the front-end engineering of OWPPs together with proper protection schemes to avoid instability incidents during operation. Fourth, industry adoption of cost-efficient HVDC solutions while acknowledging the prevailing HVDC supply chain challenges warrants substantial investigation. Last, additional emerging topics—such as grid congestion management, the optimization of grid connection capacity, and the integration of power-to-X technology, including using hydrogen as an energy storage buffer—represent the research and development areas that need deeper exploration and analysis.

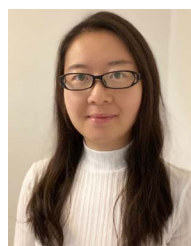
REFERENCES

- [1] "Making green energy affordable—how the offshore wind energy industry matured and what we can learn from it," 2019. Accessed: Jan. 30, 2023. [Online]. Available: <https://orsted.com/en/insights/white-papers/making-green-energy-affordable>
- [2] "GWEC. (2023, august), global offshore wind report 2023," 2023. Accessed: Oct. 30, 2023. [Online]. Available: <https://gwec.net/wp-content/uploads/2023/08/GWEC-Global-Offshore-Wind-Report-2023.pdf>
- [3] "Multi-frequency stability of converter-based modern power systems," 2024. [Online]. Available: <https://www.e-cigre.org/publications/detail/928-multi-frequency-stability-of-converter-based-modern-power-systems.html>
- [4] "GWEC. (2023, Mar.), Global offshore wind report 2023," 2024. Accessed: Oct. 30, 2023. [Online]. Available: https://gwec.net/wp-content/uploads/2023/03/GWR-2023_interactive.pdf
- [5] F. Blaabjerg and M. Ke, "Wind energy systems," *Proc. IEEE*, vol. 105, no. 11, pp. 2116–2131, Nov. 2017.
- [6] E. Istvan, S. Fekadu, F. Christian, K. Friedrich, and F. Jens, "Offshore wind power generation technologies," *Proc. IEEE*, vol. 101, no. 4, pp. 891–905, Apr. 2013.
- [7] S. W. Ali et al., "Offshore wind farm-grid integration: A review on infrastructure, challenges, and grid solutions," *IEEE Access*, vol. 9, pp. 102811–102827, 2021.
- [8] ENTSO-E, "Network code for requirements for grid connection applicable to all generators," Apr. 2016. [Online]. Available: https://www.entsoe.eu/network_codes/rfg/
- [9] Energinet, "Technical regulation 3.2.5 for wind power plants above 11 kw," 2017. [Online]. Available: <https://www.energinet.dk>
- [10] Tennet TSO GmbH, "Grid connection regulations," Feb. 2024. [Online]. Available: <https://www.tennet.eu/grid-connection-regulations>
- [11] National Grid, "Grid code - Issue 5, Revision 38," 2019. [Online]. Available: <https://www.nationalgrideso.com/document/33821/download>
- [12] EirGrid, "Eirgrid grid code," Apr. 2014. Accessed: 2019. [Online]. Available: <https://www.eirgrid.ie/grid/grid-codes-and-compliance/grid-code>

- [13] Taipower, "Technical guidelines for Taipower's grid connection of renewable generation system," Nov. 2021. [Online]. Available: <https://www.taipower.com.tw/upload/228/2023080713481796083.pdf>
- [14] Japan Electric Association, "Grid-interconnection code JEAC 9701," 2016.
- [15] NERC, "Standard PRC-024-1 – Generator frequency and voltage protective relay settings," Mar. 2014. [Online]. Available: <https://www.nerc.com/pa/Stand/Reliability%20Standards/PRC-024-1.pdf>
- [16] E. Nycander and L. Söder, "Review of European grid codes for wind farms and their implications for wind power curtailments," in *Proc. 17th Int. Wind Integration Workshop Stockholm*, 2018, pp. 1–7.
- [17] T. K. Vrana et al., "Wind power within European grid codes: Evolution, status and outlook," *Wiley Interdiscipl. Reviews: Energy Environ.*, vol. 7, no. 3, 2018, Art. no. e285.
- [18] *Wind Turbines - Part 21-1: Measurement and Assessment of Electrical Characteristics-Wind Turbines*, IEC Standard 61400-21-1, Geneva, Switzerland, 2019.
- [19] "Electromagnetic compatibility (EMC) - Part 3-7: Limits - Assessment of emission limits for the connection of fluctuating installations to MV, HV and EHV power systems," IEC, Geneva, Switzerland, Tech. Rep. 61000-3-7, 2008.
- [20] "Electromagnetic compatibility (EMC) - Part 3-6: Limits - Assessment of emission limits for the connection of distorting installations to MV, HV EHV power systems," IEC, Geneva, Switzerland, Tech. Rep. 61000-3-6, 2008.
- [21] "Wind turbines - Part 21-3: Measurement and assessment of electrical characteristics-Wind harmonic model and its application," IEC, Geneva, Switzerland, Tech. Rep. 61000-4-7, 2019.
- [22] *Grid Converter Structures for Wind Turbine Syst.*, Hoboken, NJ, USA: Wiley, 2011, ch. 6, pp. 123–143. [Online]. Available: <https://onlinelibrary.wiley.com/doi/abs/10.1002/9780470667057.ch6>
- [23] A. R. Nejad et al., "Wind turbine drivetrains: State-of-the-art technologies and future development trends," *Wind Energy Sci. Discuss.*, vol. 7, no. 1, pp. 387–411, 2022.
- [24] Y. Zhang, X. Peng, X. Yuan, Y. Li, and K. Wang, "A unidirectional cascaded high-power wind converter with reduced number of active devices," *IEEE Access*, vol. 11, pp. 10902–10911, 2023.
- [25] M. Liserre, R. Cardenas, M. Molinas, and J. Rodriguez, "Overview of multi-MW wind turbines and wind parks," *IEEE Trans. Ind. Electron.*, vol. 58, no. 4, pp. 1081–1095, Apr. 2011.
- [26] F. Blaabjerg, R. Teodorescu, M. Liserre, and A. V. Timbus, "Overview of control and grid synchronization for distributed power generation systems," *IEEE Trans. Ind. Electron.*, vol. 53, no. 5, pp. 1398–1409, Oct. 2006.
- [27] Z. Chen, J. M. Guerrero, and F. Blaabjerg, "A review of the state of the art of power electronics for wind turbines," *IEEE Trans. Power Electron.*, vol. 24, no. 8, pp. 1859–1875, Aug. 2009.
- [28] P. Rodriguez, A. V. Timbus, R. Teodorescu, M. Liserre, and F. Blaabjerg, "Flexible active power control of distributed power generation systems during grid faults," *IEEE Trans. Ind. Electron.*, vol. 54, no. 5, pp. 2583–2592, Oct. 2007.
- [29] P. Rodriguez, A. Timbus, R. Teodorescu, M. Liserre, and F. Blaabjerg, "Reactive power control for improving wind turbine system behavior under grid faults," *IEEE Trans. Power Electron.*, vol. 24, no. 7, pp. 1798–1801, Jul. 2009.
- [30] L. Xu and P. Cartwright, "Direct active and reactive power control of DFIG for wind energy generation," *IEEE Trans. Energy Convers.*, vol. 21, no. 3, pp. 750–758, Sep. 2006.
- [31] M. B. Shamsheh, R. Inzunza, I. Fukasawa, T. Tanaka, and T. Ambo, "Grid support during asymmetrical faults using negative sequence current injection," in *Proc. IEEE 4th Int. Future Energy Electron. Conf.*, 2019, pp. 1–6.
- [32] X. Liu, "Fault current negative contribution method for inverter-based distributed generators under grid unbalanced fault," *IEEE Access*, vol. 8, pp. 220807–220815, 2020.
- [33] J. Jia, G. Yang, and A. H. Nielsen, "A review on grid-connected converter control for short-circuit power provision under grid unbalanced faults," *IEEE Trans. Power Del.*, vol. 33, no. 2, pp. 649–661, Apr. 2018.
- [34] I. Karray, K. B. Kilani, and M. Elleuch, "Wind plant control under grid code requirements," in *Proc. 16th Int. Multi-Conf. Syst., Signals Devices*, 2019, pp. 706–711.
- [35] G. C. Tarnowski, P. C. Kjaer, S. Dalsgaard, and A. Nyborg, "Regulation and frequency response service capability of modern wind power plants," in *Proc. IEEE PES Gen. Meeting*, 2010, pp. 1–8.
- [36] D.-Y. Gau and Y.-K. Wu, "Overview of reactive power and voltage control of offshore wind farms," in *Proc. Int. Symp. Comput., Consum. Control*, 2020, pp. 276–279.
- [37] Y. Li, Z. Xu, J. Zhang, and K. Meng, "Variable droop voltage control for wind farm," *IEEE Trans. Sustain. Energy*, vol. 9, no. 1, pp. 491–493, Jan. 2018.
- [38] Y. Guo, H. Gao, Q. Wu, H. Zhao, J. Østergaard, and M. Shahidehpour, "Enhanced voltage control of VSC-HVDC-connected offshore wind farms based on model predictive control," *IEEE Trans. Sustain. Energy*, vol. 9, no. 1, pp. 474–487, Jan. 2017.
- [39] W. Li, M. Zhu, P. Chao, X. Liang, and D. Xu, "Enhanced FRT and postfault recovery control for MMC-HVDC connected offshore wind farms," *IEEE Trans. Power Syst.*, vol. 35, no. 2, pp. 1606–1617, Mar. 2020.
- [40] R. Teodorescu, M. Liserre, and P. Rodriguez, *Grid Converters for Photovoltaic and Wind Power Systems*. Hoboken, NJ, USA: Wiley, 2011.
- [41] J. Ma, Y. Qiu, Y. Li, W. Zhang, Z. Song, and J. S. Thorp, "Research on the impact of DFIG virtual inertia control on power system small-signal stability considering the phase-locked loop," *IEEE Trans. Power Syst.*, vol. 32, no. 3, pp. 2094–2105, May 2017.
- [42] Q.-C. Zhong and G. Weiss, "Synchronverters: Inverters that mimic synchronous generators," *IEEE Trans. Ind. Electron.*, vol. 58, no. 4, pp. 1259–1267, Apr. 2011.
- [43] Y. Lin et al., "Research roadmap on grid-forming inverters," National Renewable Energy Lab. (NREL), Golden, CO (United States), Tech. Rep. NREL/TP-5D00-73476, 2020.
- [44] M. C. Chandorkar, D. M. Divan, and R. Adapa, "Control of parallel connected inverters in standalone AC supply systems," *IEEE Trans. Ind. Appl.*, vol. 29, no. 1, pp. 136–143, Jan./Feb. 1993.
- [45] H.-P. Beck and R. Hesse, "Virtual synchronous machine," in *Proc. 9th Int. Conf. Elect. Power Qual. Utilisation*, 2007, pp. 1–6.
- [46] G.-S. Seo, M. Colombino, I. Subotic, B. Johnson, D. Groß, and F. Dörfler, "Dispatchable virtual oscillator control for decentralized inverter-dominated power systems: Analysis and experiments," in *Proc. IEEE Appl. Power Electron. Conf. Expo.*, 2019, pp. 561–566.
- [47] C. Arghir, T. Jouini, and F. Dörfler, "Grid-forming control for power converters based on matching of synchronous machines," *Automatica*, vol. 95, pp. 273–282, 2018.
- [48] A. Tayyebi, D. Groß, A. Anta, F. Kupzog, and F. Dörfler, "Frequency stability of synchronous machines and grid-forming power converters," *IEEE Trans. Emerg. Sel. Topics Power Electron.*, vol. 8, no. 2, pp. 1004–1018, Jun. 2020.
- [49] P. Denholm, T. Mai, R. W. Kenyon, B. Kroposki, and M. O'Malley, "Inertia and the power grid: A guide without the spin," Nat. Renewable Energy Lab. (NREL), Golden, CO, USA, Tech. Rep. NREL/TP-6A20-73856, 2020.
- [50] J. He and Y. W. Li, "Analysis, design, and implementation of virtual impedance for power electronics interfaced distributed generation," *IEEE Trans. Ind. Appl.*, vol. 47, no. 6, pp. 2525–2538, Nov./Dec. 2011.
- [51] R. Korte, H. Klingenberg, B. Buchholz, and A. Oudalov, "Grid forming energy storage system addresses challenges of grids with high penetration of renewables (a case study)," *CIGRE Session Mater.*, 2020.
- [52] Y. Yu, S. K. Chaudhary, S. Golestan, G. D. A. Tinajero, J. C. Vasquez, and J. M. Guerrero, "An overview of grid-forming control for wind turbine converters," in *Proc. IECON 47th Annu. Conf. Ind. Electron. Soc. IEEE*, 2021, pp. 1–6.
- [53] A. Attya, J. L. Dominguez-Garcia, and O. Anaya-Lara, "A review on frequency support provision by wind power plants: Current and future challenges," *Renewable Sustain. Energy Rev.*, vol. 81, pp. 2071–2087, 2018.
- [54] J. Aho et al., "A tutorial of wind turbine control for supporting grid frequency through active power control," in *Proc. Amer. Control Conf.*, 2012, pp. 3120–3131.
- [55] A. Mullane and M. O'malley, "The inertial response of induction-machine-based wind turbines," *IEEE Trans. Power Syst.*, vol. 20, no. 3, pp. 1496–1503, Aug. 2005.
- [56] J. Morren, S. W. D. Haan, W. L. Kling, and J. Ferreira, "Wind turbines emulating inertia and supporting primary frequency control," *IEEE Trans. Power Syst.*, vol. 21, no. 1, pp. 433–434, Feb. 2006.
- [57] F. Gonzalez-Longatt, E. Chikuni, and E. Rashayi, "Effects of the synthetic inertia from wind power on the total system inertia after a frequency disturbance," in *Proc. IEEE Int. Conf. Ind. Technol.*, 2013, pp. 826–832.

- [58] A. Junyent-Ferr, Y. Pipelzadeh, and T. C. Green, "Blending HVDC-link energy storage and offshore wind turbine inertia for fast frequency response," *IEEE Trans. Sustain. Energy*, vol. 6, no. 3, pp. 1059–1066, Jul. 2015.
- [59] R. Eriksson, N. Modig, and K. Elkington, "Synthetic inertia versus fast frequency response: A definition," *IET Renewable Power Gener.*, vol. 12, no. 5, pp. 507–514, 2018.
- [60] M. Adibi et al., "Power system restoration-a task force report," *IEEE Trans. Power Syst.*, vol. 2, no. 2, pp. 271–277, May 1987.
- [61] G.-S. Seo, "Paradigm shift: Black start from inverter-based resources-IBR-driven power system black start," Nat. Renewable Energy Lab.(NREL), Golden, CO, USA, Tech. Rep. NREL/PR-5D00-82258, 2022.
- [62] J. Jia, G. Yang, A. H. Nielsen, E. Muljadi, P. Weinreich-Jensen, and V. Gevorgian, "Synchronous condenser allocation for improving system short circuit ratio," in *Proc. 5th Int. Conf. Electric Power Energy Convers. Syst.*, 2018, pp. 1–5.
- [63] J. Sawant, G.-S. Seo, and F. Ding, "Resilient inverter-driven black start with collective parallel grid-forming operation," in *Proc. IEEE Innov. Smart Grid Technol. Conf.*, 2023, pp. 1–5.
- [64] A. Banerjee et al., "Autonomous microgrid restoration using grid-forming inverters and smart circuit breakers," in *Proc. IEEE Power Energy Soc. Gen. Meeting*, 2022, pp. 1–5.
- [65] M. Aktarujjaman, M. Kashem, M. Negnevitsky, and G. Ledwich, "Black start with DFIG based distributed generation after major emergencies," in *Proc. Int. Conf. Power Electron., Drives Energy Syst.*, 2006, pp. 1–6.
- [66] L. Yu, R. Li, and L. Xu, "Distributed PLL-based control of offshore wind turbines connected with diode-rectifier-based HVDC systems," *IEEE Trans. Power Del.*, vol. 33, no. 3, pp. 1328–1336, Jun. 2018.
- [67] "TNO report: Large offshore wind harmonics mitigation (LOW-HarM) - final summary report," 2019. [Online]. Available: <https://projecten.topsectorenergie.nl/storage/app/uploads/public/613/5d4/e41/6135d4e412485508377080.pdf>
- [68] *Electromagnetic Compatibility (EMC) – Part 4-7: Testing and Measurement Techniques—General Guide on Harmonics and Interharmonics Measurements and Instrumentation, for Power Supply Systems and Equipment Connected Thereto*, IEC Standard 61000-4-7:2009, IEC, Geneva, Switzerland, 2009.
- [69] J. Arrillaga and N. Watson, "Power System Harmonics," Hoboken, NJ, USA: Wiley, 2003.
- [70] J. Lei, Z. Qin, W. Li, P. Bauer, and X. He, "Stability region exploring of shunt active power filters based on output admittance modeling," *IEEE Trans. Ind. Electron.*, vol. 68, no. 12, pp. 12130–12140, Dec. 2021.
- [71] L. Kocewiak, B. Kramer, O. Holmström, K. Jensen, and L. Shuai, "Resonance damping in array cable systems by wind turbine active filtering in large offshore wind power plants," *IET Renewable Power Gener.*, vol. 11, no. 7, pp. 1069–1077, 2017.
- [72] E. Guest, K. Jensen, and T. Rasmussen, "Mitigation of harmonic voltage amplification in offshore wind power plants by wind turbines with embedded active filters," *IEEE Trans. Sustain. Energy*, vol. 11, no. 2, pp. 785–794, Apr. 2020.
- [73] L. Kocewiak et al., "Active filtering trial to reduce harmonic voltage distortion in an offshore wind power plant," in *Proc. 22nd Wind Sol. Integration Workshop*, 2023, pp. 394–399.
- [74] X. Wang and F. Blaabjerg, "Harmonic stability in power electronic-based power systems: Concept, modeling, and analysis," *IEEE Trans. Smart Grid*, vol. 10, no. 3, pp. 2858–2870, May 2019.
- [75] L. Larumbe, Z. Qin, and P. Bauer, "Guidelines for stability analysis of the DDSRF-PLL using LTI and LTP modelling in the presence of imbalance," *IEEE Open J. Ind. Electron. Soc.*, vol. 3, pp. 339–352, 2022.
- [76] L. Larumbe, Z. Qin, L. Wang, and P. Bauer, "Impedance modeling for three-phase inverters with double synchronous reference frame current controller in the presence of imbalance," *IEEE Trans. Power Electron.*, vol. 37, no. 2, pp. 1461–1475, Feb. 2022.
- [77] U. Topcu, A. Packard, P. Seiler, and T. Wheeler, "Stability region analysis using simulations and sum-of-squares programming," in *Proc. Amer. Control Conf.*, New York, NY, USA, 2007, pp. 6009–6014.
- [78] M. Kaban, P. Singh, and D. Niebur, "Large signal Lyapunov-based stability studies in microgrids: A review," *IEEE Trans. Smart Grid*, vol. 8, no. 5, pp. 2287–2295, Sep. 2017.
- [79] K. Meng, W. Zhang, J. Qiu, Y. Zheng, and Z. Y. Dong, "Offshore transmission network planning for wind integration considering AC and DC transmission options," *IEEE Trans. Power Syst.*, vol. 34, no. 6, pp. 4258–4268, Nov. 2019.
- [80] D. Elliott et al., "A comparison of ac and HVDC options for the connection of offshore wind generation in Great Britain," *IEEE Trans. Power Del.*, vol. 31, no. 2, pp. 798–809, Apr. 2016.
- [81] C.-J. Chou, Y.-K. Wu, G.-Y. Han, and C.-Y. Lee, "Comparative evaluation of the HVDC and HVAC links integrated in a large offshore wind farm—an actual case study in Taiwan," *IEEE Trans. Ind. Appl.*, vol. 48, no. 5, pp. 1639–1648, Sep./Oct. 2012.
- [82] J. Hjerrild et al., "Hornsea projects one and two—design and execution of the grid connection for the world's largest offshore wind farms," in *Proc. Cigre Symp. Aalborg*, 2019, pp. 1–6.
- [83] J. Dakic, M. Cheah-Mane, O. Gomis-Bellmunt, and E. Prieto-Araujo, "Hvac transmission system for offshore wind power plants including mid-cable reactive power compensation: Optimal design and comparison to VSC-HVDC transmission," *IEEE Trans. Power Del.*, vol. 36, no. 5, pp. 2814–2824, Oct. 2021.
- [84] J. Song-Manguelle, M. H. Todorovic, S. Chi, S. K. Gunturi, and R. Datta, "Power transfer capability of HVAC cables for subsea transmission and distribution systems," *IEEE Trans. Ind. Appl.*, vol. 50, no. 4, pp. 2382–2391, Jul./Aug. 2014.
- [85] T. Zhao, Y. Li, X. Pan, P. Wang, and J. Zhang, "Real-time optimal energy and reserve management of electric vehicle fast charging station: Hierarchical game approach," *IEEE Trans. Smart Grid*, vol. 9, no. 5, pp. 5357–5370, Sep. 2018.
- [86] J. Ruddy, R. Meere, C. O'Loughlin, and T. O'Donnell, "Design of VSC connected low frequency AC offshore transmission with long HVAC cables," *IEEE Trans. Power Del.*, vol. 33, no. 2, pp. 960–970, Apr. 2018.
- [87] "BorWin1." Accessed: Jan. 2, 2023. [Online]. Available: <https://www.tennet.eu/projects/borwin1>
- [88] "About the dogger bank wind farm projects," May 2020, Accessed: Jan. 2, 2023. [Online]. Available: <https://doggerbank.com/about/>
- [89] "Hornsea 3: World's single largest offshore wind farm." Accessed: Apr. 03, 2024. [Online]. Available: <https://www.hitachienergy.com/about-us/customer-success-stories/hornsea-3>
- [90] A. Lesnicar and R. Marquardt, "An innovative modular multilevel converter topology suitable for a wide power range," in *Proc. IEEE Bologna Power Tech Conf. Proc.*, 2004, pp. 1–6.
- [91] V. F. Lescale, P. Holmberg, R. Ottersten, and Y. J. Häfner, "Paralleling offshore wind farm HVDC ties on offshore side," *CIGRE*, pp. 1–11, 2012.
- [92] R. Li, L. Yu, L. Xu, and G. P. Adam, "Coordinated control of parallel DR-HVDC and MMC-HVDC systems for offshore wind energy transmission," *IEEE J. Emerg. Sel. Top. Power Electron.*, vol. 8, no. 3, pp. 2572–2582, Sep. 2020.
- [93] "PROMOTioN - home," Jan. 2021, accessed: Jan. 2, 2023. [Online]. Available: <https://www.promotion-offshore.net/>
- [94] D. V. Hertem and M. Ghandhari, "Multi-terminal VSC HVDC for the European supergrid: Obstacles," *Renewable Sustain. Energy Rev.*, vol. 14, no. 9, pp. 3156–3163, Dec. 2010.
- [95] F. Mazzoldi, J. Taisne, C. Martin, and B. Rowe, "Adaptation of the control equipment to permit 3-terminal operation of the HVDC link between Sardinia, Corsica and Mainland Italy," *IEEE Power Eng. Rev.*, vol. 9, no. 4, pp. 87–87, Apr. 1989.
- [96] X. Li, Z. Yuan, J. Fu, Y. Wang, T. Liu, and Z. Zhu, "Nanao multi-terminal VSC-HVDC project for integrating large-scale wind generation," in *Proc. IEEE PES Gen. Meeting Conf. Expo.*, 2014, pp. 1–5.
- [97] X. Li, Z. Yuan, J. Fu, Y. Wang, T. Liu, and Z. Zhu, "Nanao multi-terminal VSC-HVDC project for integrating large-scale wind generation," *Proc. IEEE PES Gen. Meeting Conf. Exp.*, 2014, pp. 1–5.
- [98] H. Pang and X. Wei, "Research on key technology and equipment for zhangbei 500kv DC grid," in *Proc. IEEE Int. Power Electron. Conf.*, 2018, pp. 2343–2351.
- [99] "Hitachi energy's HVDC technology supports ssen transmission in taking another step towards their commitment to powering 10 million UK homes with renewable energy in 2026 by enabling the harvesting of Scotland's renewable energy potential." Accessed: Feb. 7, 2024. [Online]. Available: <https://www.hitachienergy.com/ch/de/about-us/customer-success-stories/shetland>

- [100] S. Gang, P. Simin, C. Xu, C. Zhe, and H. Wei, "Grid integration of offshore wind farms and offshore oil/gas platforms," in *Proc. 7th Int. Power Electron. Motion Control Conf.*, 2012, pp. 1301–1305.
- [101] S. Sanchez, A. Garces, G. Bergna-Diaz, and E. Tedeschi, "Dynamics and stability of meshed multiterminal HVDC networks," *IEEE Trans. Power Syst.*, vol. 34, no. 3, pp. 1824–1833, May 2019.
- [102] H. Li, C. Liu, G. Li, and R. Iravani, "An enhanced DC voltage droop-control for the VSC-HVDC grid," *IEEE Trans. Power Syst.*, vol. 32, no. 2, pp. 1520–1527, Mar. 2017.
- [103] F. Thams, R. Eriksson, and M. Molinas, "Interaction of droop control structures and its inherent effect on the power transfer limits in multiterminal VSC-HVDC," *IEEE Trans. Power Del.*, vol. 32, no. 1, pp. 182–192, Feb. 2017.
- [104] E. Prieto-Araujo, A. Egea-Alvarez, S. Fekiasl, and O. Gomis-Bellmunt, "DC voltage droop control design for multiterminal HVDC systems considering AC and DC grid dynamics," *IEEE Trans. Power Del.*, vol. 31, no. 2, pp. 575–585, Apr. 2016.
- [105] O. Kuhn et al., "2nd generation DC grid access for offshore wind farms: HVDC in an AC fashion," in *Proc. CIGRE*, 2016, pp. 1–7.
- [106] S. Seman, R. Zurowski, and C. Taratoris, "Interconnection of advanced type 4 WTGS with diode rectifier based HVDC solution and weak ac grids," in *Proc. 14th Wind Integration Workshop*, Brussels, Belgium, 2015, pp. 1–7.
- [107] O. Kuhn et al., "2nd generation DC grid access for offshore wind farms: HVDC in an ac fashion," in *Proc. CIGRE*, 2016, pp. 1–7.
- [108] S. Seman, R. Zurowski, and C. Taratoris, "Interconnection of advanced type 4 WTGS with diode rectifier based HVDC solution and weak AC grids," in *Proc. 14th Wind Integration Workshop*, Brussels, Belgium, 2015, pp. 1–7.
- [109] W. Lin, J. Wen, M. Yao, S. Wang, S. Cheng, and N. Li, "Series VSC-LCC converter with self-commutating and dc fault blocking capabilities," in *Proc. IEEE PES Gen. Meeting Conf. Expo.*, 2014, pp. 1–5.
- [110] T. H. Nguyen, D.-C. Lee, and C.-K. Kim, "A series-connected topology of a diode rectifier and a voltage-source converter for an HVDC transmission system," *IEEE Trans. Power Electron.*, vol. 29, no. 4, pp. 1579–1584, Apr. 2014.
- [111] T. H. Nguyen, Q. A. Le, and D.-C. Lee, "A novel HVDC-link based on hybrid voltage-source converters," in *Proc. IEEE Energy Convers. Congr. Expo.*, 2015, pp. 3338–3343.
- [112] J. L. Rodriguez-Amendedo, S. Arnaltes-Gomez, M. Aragues-Penalba, and O. Gomis-Bellmunt, "Control of the parallel operation of VSC-HVDC links connected to an offshore wind farm," *IEEE Trans. Power Deliv.*, vol. 34, no. 1, pp. 32–41, Feb. 2019.
- [113] Y. Chang and X. Cai, "Hybrid topology of a diode-rectifier-based HVDC system for offshore wind farms," *IEEE J. Emerg. Sel. Top. Power Electron.*, vol. 7, no. 3, pp. 2116–2128, Sep. 2019.
- [114] Y. Jing, R. Li, L. Xu, and Y. Wang, "Enhanced AC voltage and frequency control of offshore MMC station for wind farm connection," *IET Renewable Power Gen.*, vol. 12, no. 15, pp. 1771–1777, Nov. 2018.
- [115] R. Vidal-Albalade, H. Beltran, A. Rolan, E. Belenguer, R. Pena, and R. Blasco-Gimenez, "Analysis of the performance of MMC under fault conditions in HVDC-based offshore wind farms," *IEEE Trans. Power Del.*, vol. 31, no. 2, pp. 839–847, Apr. 2016.
- [116] L. Kunjumammed, B. Pal, R. Gupta, and K. Dykes, "Stability analysis of a PMSG-based large offshore wind farm connected to a VSC-HVDC," in *Proc. IEEE Power Energy Soc. Gen. Meeting*, 2018, pp. 1–11.
- [117] R. Blasco-Gimenez, S. Ano-Villalba, J. Rodriguez-D'Erlee, S. Bernal-Perez, and F. Morant, "Diode-based HVDC link for the connection of large offshore wind farms," *IEEE Trans. Energy Convers.*, vol. 26, no. 2, pp. 615–626, Jun. 2011.
- [118] S. Bernal-Perez, S. Ano-Villalba, R. Blasco-Gimenez, and J. Rodriguez-D'Erlee, "Efficiency and fault ride-through performance of a diode-rectifier- and VSC-inverter-based HVDC link for offshore wind farms," *IEEE Trans. Ind. Electron.*, vol. 60, no. 6, pp. 2401–2409, Jun. 2013.
- [119] C. Prignitz, H.-G. Eckel, and A. Rafoth, "FixReF sinusoidal control in line side converters for offshore wind power generation," in *Proc. IEEE 6th Int. Symp. Power Electron. Distrib. Gener. Syst.*, 2015, pp. 1–5.
- [120] C. Prignitz, H.-G. Eckel, and H.-J. Knaak, "Voltage and current behavior in a FixReF controlled offshore wind farm using a HVDC transmission system based on uncontrolled diode rectifier units," in *Proc. IEEE 18th Eur. Conf. Power Electron. Appl.*, 2016, pp. 1–6.
- [121] B. Liu, J. Xu, R. E. Torres-Olguin, and T. Undeland, "Faults mitigation control design for grid integration of offshore wind farms and oil & gas installations using VSC HVDC," in *Proc. IEEE SPEEDAM*, 2010, pp. 792–797.
- [122] U. Karaagac, J. Mahseredjian, L. Cai, and H. Saad, "Offshore wind farm modeling accuracy and efficiency in MMC-based multiterminal HVDC connection," *IEEE Trans. Power Del.*, vol. 32, no. 2, pp. 617–627, Apr. 2017.
- [123] L. Zhang, L. Harnefors, and H.-P. Nee, "Power-synchronization control of grid-connected voltage-source converters," *IEEE Trans. Power Syst.*, vol. 25, no. 2, pp. 809–820, May 2010.
- [124] S. Alepuz et al., "Control strategies based on symmetrical components for grid-connected converters under voltage dips," *IEEE Trans. Ind. Electron.*, vol. 56, no. 6, pp. 2162–2173, Jun. 2009.
- [125] D. Roio, R. I. Bojoi, L. R. Limongi, and A. Tenconi, "New stationary frame control scheme for three-phase PWM rectifiers under unbalanced voltage dips conditions," *IEEE Trans. Ind. Appl.*, vol. 46, no. 1, pp. 268–277, Jan./Feb. 2010.
- [126] T. Neumann, T. Wijnhoven, G. Deconinck, and I. Erlich, "Enhanced dynamic voltage control of type 4 wind turbines during unbalanced grid faults," *IEEE Trans. Energy Convers.*, vol. 30, no. 4, pp. 1650–1659, Dec. 2015.
- [127] L. Shi, G. Adam, R. Li, and L. Xu, "Control of offshore MMC during asymmetric offshore AC faults for wind power transmission," *IEEE J. Emerg. Sel. Topic Power Electron.*, vol. 8, no. 2, pp. 1074–1083, Jun. 2020.
- [128] C. Nentwig, J. Haubrock, R. H. Renner, and D. V. Hertem, "Application of DC choppers in HVDC grids," in *Proc. IEEE Int. Energy Conf.*, 2016, pp. 1–5.
- [129] S. Nanou and S. Papathanassiou, "Evaluation of a communication-based fault ride-through scheme for offshore wind farms connected through high-voltage DC links based on voltage source converter," *IET Renew. Power Gen.*, vol. 9, no. 8, pp. 882–891, Nov. 2015.
- [130] M. A. Ahmed and Y. C. Kim, "Hierarchical communication network architectures for offshore wind power farms," in *Proc. Int. Symp. Comput., Consum. Control*, 2014, vol. 7, pp. 3420–3437.
- [131] B. Silva, C. L. Moreira, H. Leite, and J. A. P. Lopes, "Control strategies for AC fault ride through in multiterminal HVDC grids," *IEEE Trans. Power Del.*, vol. 29, no. 1, pp. 395–405, Feb. 2014.



DAN WU (Senior Member, IEEE) received the B.Sc. (Hons.) and M.Sc. (Hons.) degrees in electrical engineering from the Beijing Institute of Technology (BIT), Beijing, China, in 2009 and 2012, respectively, and the Ph.D. degree in electrical engineering from Aalborg University, Aalborg, Denmark, in 2015. In 2016, she joined industry and was with Vestas Wind Power A/S, Siemens Gamesa Renewable Energy, and she is currently a Senior Electrical Engineer at Shell Global Solution b.v., where she is also the technical focal

point on grid-forming technology. She is specialized on grid integration of power electronics, including converter control, power plant control, grid compliance. She has more than 20 journal and conference publications, six international patents, and gained a lot of project experiences on these aspects. She is leading from Shell side and collaborating with Energinet and other industrial partners on the project Deployment of Grid Forming Technology in the Danish Power System. She is/was also involved in projects as Formosa II, Moray West, Greater Changhua, Atlantic Shore Ph1, MunmuBaram. Dr. Dan Wu is Associate Editor for IEEE TRANSACTIONS ON SMART GRID, and active member of IEEE Power Electronics Society and Energy Society, IEEE Industrial Electronics Society and Cigre B4 Study Committee.



GAB-SU SEO (Senior Member, IEEE) received the Ph.D. degree in electrical engineering from Seoul National University, Seoul, South Korea, in 2015. From 2016 to 2017, he was a Research Associate with the Colorado Power Electronics Center, University of Colorado, Boulder, CO, USA. Since 2018, he has been with the Power Systems Engineering Center, National Renewable Energy Laboratory (NREL), Golden, CO, USA, where he is currently a Senior Electrical Engineer and leads research projects focused on power electronics

and power systems applications for electric grids with high integrations of inverter-based resources. He has coauthored more than 80 IEEE journal and peer-reviewed conference papers and was the recipient of one IEEE Best Paper Award. He coauthored the Research Roadmap on Grid-Forming Inverters (NREL, 2020). His current research interests include power electronics for renewable energy systems and microgrids and power systems engineering for grid modernization, including grid-forming inverter control and inverter-driven power systems black start for low- or zero-inertia grids to improve grid resilience and stability. Dr. Seo is an IEEE Roadmap Working Group Chair of the International Technology Roadmap of Power Electronics for Distributed Energy Resources (ITRD)—WG3 Integration and Control of DERs. He is an Associate Editor of IEEE TRANSACTIONS ON POWER ELECTRONICS, IEEE TRANSACTIONS ON INDUSTRY APPLICATIONS, the IEEE OPEN JOURNAL OF POWER ELECTRONICS, and the *Journal of Power Electronics*. He is currently the Secretary of the IEEE Power Electronics Society Technical Committee on Sustainable Energy Systems (IEEE PELS TC5) and the Vice Chair of the IEEE PELS Denver Section.



LUKASZ KOCEWIAK (Senior Member, IEEE) received the B.Sc. and M.Sc. degrees in electrical engineering from the Warsaw University of Technology, Warsaw, Poland, in 2007, and the Ph.D. degree from Aalborg University, Aalborg, Denmark, in 2012. He is currently with Ørsted and is working as a Digital Product Manager. He is a Power System Specialist within the area of design of electrical infrastructure in large offshore wind power plants. He is the author and co-author of more than 100 publications. His research interests

include harmonics, stability and nonlinear dynamics in power electronics and power systems especially focused on wind power generation units. He is a member of various working groups and activities within Cigré and IEC.



YIN SUN (Member, IEEE) received the B.Sc. degree in electrical engineering from the Harbin Institute of Technology, Harbin, China, in 2008, the M.Sc. degree in sustainable energy technology from Twente University, the Netherlands, in 2010 and the Ph.D. degree in stability and control of the power electronics dominant grid from the Eindhoven University of Technology, the Netherlands, 2018. He is currently a Senior Electrical Engineer and Technology Manager for grid connection technology at Shell, Subject Matter Expert (SME) of

power system analysis, HVDC and power converters with Instrument Control and Electrical (ICE) Discipline, Shell Projects& Technology. He is a part-time Associate Professor focusing on grid connection technology, Electrical Energy System Group, Eindhoven University of Technology.



LIE XU (Senior Member, IEEE) received the B.Sc. degree in mechatronics from Zhejiang University, Hangzhou, China, in 1993, and the Ph.D. degree in electrical engineering from the University of Sheffield, Sheffield, U.K., in 2000. He is currently a Professor with the Department of Electronic & Electrical Engineering, University of Strathclyde, Glasgow, U.K. He was with the Queen's University of Belfast and ALSTOM T&D, Stafford, U.K. His research interests include power electronics, wind energy generation and grid integration, and appli-

cation of power electronics to power systems, such as HVDC and MVDC systems for power transmission and distribution.



ZIAN QIN (Senior Member, IEEE) received the B.Sc. degree in electrical engineering from Beihang University, Beijing, China, in 2009, the M.Sc. degree in electrical engineering from the Beijing Institute of Technology, Beijing, China, in 2012, and the Ph.D. degree in electrical engineering from Aalborg University, Aalborg, Denmark, in 2015. He is currently an Associate Professor with the Department of Electrical Sustainable Energy, Delft University of Technology, the Netherlands. In 2014, he was a Visiting Scientist with

RWTH Aachen University, Aachen, Germany. He has more than 100 journals/conference papers, four book chapters, and two international patents, and he has worked on several European, Dutch national and industrial projects in his research field, which include power quality and stability of power electronics-based grids, solid-state transformers, and battery energy storage. He is the Dutch national representative in Cigré Working Group B4.101 on grid forming energy storage systems. He is as an Associate Editor for IEEE TRANSACTIONS ON INDUSTRIAL ELECTRONICS, a Guest Associate Editor of IEEE JOURNAL OF EMERGING AND SELECTED TOPICS and IEEE TRANSACTIONS ON ENERGY CONVERSION. He is a Distinguished Reviewer for 2020 of IEEE TRANSACTIONS OF INDUSTRIAL ELECTRONICS. He was the Technical Program Chair of IEEE-PEDG 2024, IEEE-PEDG 2023, IEEE-ISIE 2020, IEEE-COMPEL 2020. He is the winner of the Excellent Innovation Award, 2nd Place, in the IEEE International Challenge in Design Methods for Power Electronics.



CHI SU received the B.Eng. and M.Sc. degrees in electrical engineering from the Huazhong University of Science and Technology, Wuhan, China, in 2003 and 2007 respectively, and the Ph.D. degree in electrical engineering from Aalborg University, Aalborg, Denmark, in 2012. He is currently an R&D Engineer with the Frequency Domain and EMT Modeling team at Siemens Gamesa Renewable Energy A/S. His research mainly focuses on stability and harmonic analysis and relevant model development in the wind turbine system.